bioRxiv preprint doi: https://doi.org/10.1101/2020.10.19.346049; this version posted October 19, 2020. The copyright holder for this preprint (which was not certified by peer review) is the author/funder. All rights reserved. No reuse allowed without permission.

To *Plant Physiology*

Short title

Role of GPI-anchor on AGP transport and maturation

Correspondence to:
Ken Matsuoka
Department of Bioscience and Biotechnology, Faculty of Agriculture
Kyushu University
744 Motooka, Nishi-ku, Fukuoka 819-0395, Japan.
e-mail: kenmat@agr.kyushu-u.ac.jp
fax: +81-92-802-4713

Title

GPI-anchoring is required for the proper transport and glycosylation of arabinogalactan protein precursor

Author names and affiliations
Daiki Nagasato[1], Yuto Sugita[1], Yuhei Tsuno[1], Rutsuko Tanaka[2], Ken Matsuoka[1,3]

1. Department of Bioscience and Biotechnology, Graduate School of Bioresource and Bioenvironmental Science, Kyushu University
2. Chikushigaoka High School
3. Department of Bioscience and Biotechnology, Faculty of Agriculture, Kyushu University

Footnotes

List of author contributions

Y.T., R.T. and K.M. performed the experiments on GFP-fusion proteins; D.N. and Y.S. performed the experiments on sporamin-fusion proteins; D.N., Y.T., Y.S. and K.M.

bioRxiv preprint doi: https://doi.org/10.1101/2020.10.19.346049; this version posted October 19, 2020. The copyright holder for this preprint (which was not certified by peer review) is the author/funder. All rights reserved. No reuse allowed without permission.

designed the experiments and analyzed the data; K.M. conceived the project and wrote the article with contributions from all the authors.

Funding information

This work was supported in part by JSPS KAKENHI Grant Number 26292194 to K.M. from the Japan Society for the Promotion of Science.

E-mail address of Ken Matasuoka, the author for contact: kenmat@agr.kyushu-u.ac.jp

bioRxiv preprint doi: https://doi.org/10.1101/2020.10.19.346049; this version posted October 19, 2020. The copyright holder for this preprint (which was not certified by peer review) is the author/funder. All rights reserved. No reuse allowed without permission.

Abstract

Arabinogalactan proteins (AGPs) are extracellular proteoglycans with many O-linked glycan chains. Precursors to many AGPs contain a C-terminal signal for the addition of a GPI-anchor, yet the role of this modification has not been elucidated. NtAGP1, a tobacco precursor to AGP, comprises a signal peptide, an AGP-coding region and a GPI-anchoring signal, and classified as a member of classical AGP. Using green fluorescent protein (GFP) and sweet potato sporamin (SPO) as tags and tobacco BY-2 cells as the host, we analyzed the transport and modification of NtAGP1. The fusion protein of GFP or SPO and NtAGP1 expressed in BY-2 cells migrated as a large smear on SDS-polyacrylamide gel. Confocal microscopic analysis indicated that the GFP and NtAGP1 fusion protein localized to the plasma membrane (PM), and fractionation studies of microsomes indicated that the majority of the fusion protein of SPO and NtAGP1 (SPO-AGP) localized to the PM. In contrast, the expression of mutants without a GPI-anchoring signal yielded several forms, and the largest forms migrating as large smears on the gel were secreted into the culture medium, whereas other forms were recovered in the endomembrane organelles. Comparison of the glycan structures of the SPO-AGP recovered in microsomes and the secreted mutant SPO-AGP without a GPI-anchoring signal using antibodies against AGP glycan epitopes indicated that the glycan structures of these proteins are different. These observations indicated that a GPI-anchoring signal is required for both the proper transport and glycosylation of the AGP precursor.

Introduction

Arabinogalactan proteins (AGPs) are plant cell wall proteoglycans with diverse functions (Pereira et al., 2015). Most of them contain many arabinogalactan (AG)-type glycan chains attached to Hyp residues that are post-translationally generated by the action of prolyl hydroxylases (Showalter et al., 2010). These proteins are classified into at least 5 groups based on their domain composition (Showalter et al., 2010). One of these groups consists of precursors to the classical AGPs; each of these precursors is made up of a signal peptide for the translocation of the endoplasmic reticulum (ER) membrane, glycosylation domains with many proline residues, and a signal sequence for the attachment of a glycosylphosphatidylinositol (GPI) anchor (Showalter et al., 2010).

GPI-anchor is a class of lipid anchors that retain proteins at the surface of the plasma membrane (PM), especially within the sphingolipid-sterol rich lipid domain

bioRxiv preprint doi: https://doi.org/10.1101/2020.10.19.346049; this version posted October 19, 2020. The copyright holder for this preprint (which was not certified by peer review) is the author/funder. All rights reserved. No reuse allowed without permission.

(Liu and Fujita, 2020). Based on analyses of mammalian cells and baker's yeast, it has been proposed that the biosynthesis of GPI-anchors and their subsequent modification during transport to the PM proceed as follows. First, biosynthesis of the GPI-anchor starts at the ER, and then the pre-assembled GPI-anchor is transferred from the ER to the carboxy-terminus of proteins that contain the GPI-anchoring signal to yield a GPI-anchored protein. During the subsequent transport to the PM by passing through the Golgi apparatus, the lipid part of the anchor undergoes remodeling and changes its structure (Liu and Fujita, 2020). Most of the orthologs of genes that are dispensable for the biosynthesis and remodeling of GPI-anchors in mammals and yeast are found in higher plants. However, few of the genes that are predicted to be involved in this step have been characterized to date, as their null mutants are embryo lethal (Yeats et al., 2018).

The biosynthesis of AG glycan on AGP starts at the ER and *cis*-side of the Golgi apparatus, where Pro residues are converted to Hyp residues by the action of prolyl-hydroxylases localized in the ER and *cis*-side of the Golgi apparatus (Yuasa et al., 2005; Velasquez et al., 2015; Parsons et al., 2018). Subsequent addition of galactose to the Hyp residue by Hyp galactosyltransferases (Oka et al., 2010; Basu et al., 2013, 2015; Ogawa-Ohnishi and Matsubayashi, 2015) and building of AG glycan on the galactose residue in the Golgi apparatus allows maturation of the AGP precursor (reviewed in Showalter and Basu, 2106). During or after maturation, glycosylated and GPI-anchored AGPs are transported to the PM, and some of them are released to the extracellular space by the action of phospholipase in the cell wall. Several enzymes involved in AGP glycan synthesis have been characterized (reviewed in Showalter and Basu, 2016), but such enzymes have not yet been characterized completely based on the structure of the AGP glycans from tobacco BY-2 cells and Arabidopsis (Tan et al., 2004; Tryfona et al., 2015; Showalter and Basu, 2016).

As both the remodeling of the GPI-anchors and maturation of AGP glycans takes place in the Golgi apparatus, there may be a linkage between these two modifications. The Golgi apparatus is an organelle located in the endomembrane transport system, and this system directs proteins to several destinations including the PM, extracellular space and vacuoles. As such, GPI-anchoring might play a role in the proper transport of proteins. However, this possibility has not been adequately investigated, especially with respect to the transport of AGP. It has been reported that GPI-anchoring is dispensable for PM localization of the Citrin-fused FLA4 protein, a fasciclin-domain containing AGP in Arabidopsis (Xue et al., 2017). In this case, most of the green fluorescence of the mutant Citrin-FLA4 lacking a GPI-anchoring signal appeared to be

bioRxiv preprint doi: https://doi.org/10.1101/2020.10.19.346049; this version posted October 19, 2020. The copyright holder for this preprint (which was not certified by peer review) is the author/funder. All rights reserved. No reuse allowed without permission.

retained in the ER, and only a part of the green fluorescence from this protein seemed to be secreted to the extracellular space, although this partial secretion was sufficient to complement the mutant phenotype of fla4 (Xue et al., 2017). Although this observation indicates that GPI-anchoring is required for the proper localization of this protein, this observation may not be applied to other classes of AGP; for example, classical AGP, which does not contain a fasciclin-domain and almost all of the mature polypeptide region is predicted to be heavily glycosylated with AG glycans (Showalter et al., 2010).

Here we investigated the role of GPI-anchoring on the transport and glycosylation of tobacco NtAGP1 (GenBank BAU61512), which is a classical AGP expressed in tobacco BY-2 cells, by expressing two different protein-tagged versions in tobacco BY-2 cells. We present evidence that GPI-anchoring is required for both the proper transport and the proper glycosylation of this protein.

Results

Expression of the GFP-NtAGP1 fusion protein and its mutant without a GPI-anchoring signal in tobacco BY2-cells

The precursor to NtAGP1 consists of 132 amino acids; a signal peptide of 21 amino acids, a glycosylation domain of 86 amino acids and a GPI-anchoring signal of 25 amino acids. Within the glycosylation region there are 23 Pro residues, all of which are surrounded with amino acids that make up the targeting sites for prolyl hydroxylases (Shimizu et al., 2005). Among these proline residues, 15 fit to the arabinogalactosylation site (Shimizu et al., 2005), and the remaining 8 are contiguous prolines that might form the site for the attachment of oligo-arabinose (Xu et al., 2008). Because most of the distances between the proline residues in NtAGP1 are equal to or less than 5 amino acids, and because the minimum length of a peptide epitope is 6 amino acid residues (Singh et al., 2013), we thought that it would be almost impossible to generate an antibody against the peptide sequence of NtAGP1 to detect the native protein in tobacco tissues and cells. We thus adopted the alternative approach of expressing fusion proteins consisting of NtAGP1 and protein tags and characterizing these proteins in tobacco BY-2 cells.

We first generated a construct for the expression of a fusion protein containing green fluorescence protein (GFP) between the signal peptide and the subsequent region of NtAGP1 (GFP-AGP). We also generated a mutant of this protein without a GPI-anchoring signal (GFP-AGPΔC) and a signal peptide with GFP only (GFP)

bioRxiv preprint doi: https://doi.org/10.1101/2020.10.19.346049; this version posted October 19, 2020. The copyright holder for this preprint (which was not certified by peer review) is the author/funder. All rights reserved. No reuse allowed without permission.

(Fig.1A). These proteins as well as the fusion proteins of the PM water channel and GFP (PIP-GFP: Yamauchi et al., 2003) were expressed in tobacco BY-2 cells, and the resulting transformed cells were cultured in suspension. We then analyzed the GFP fluorescence of proteins in these transformed cell cultures that were grown for either 3 days (to the logarithmic growth phase) or 7 days (to the stationary growth phase) after separation of proteins by SDS-PAGE and fluorescence recording (Fig. 1B). The fluorescence of GFP-AGP migrated as a large smear at around the 200 kDa position, and the intensity of this signal was stronger at 7 days. In the case of GFP-AGPΔC, at least three smear bands were observed: two bands that migrated to the 120 kDa and 48 kDa positions, and a relatively sharp band that migrated to around the 37 kDa position, the size of which corresponded to the non-glycosylated form of this approximately 35-kDa protein (Fig. 1B). Among these proteins, the largest form migrated more slowly at 7 days than that at 3 days on the SDS-polyacrylamide gel. The control proteins, GFP and PIP-GFP, migrated to the corresponding position on the SDS-polyacrylamide gel, as expected.

To determine the localization of these GFP-fusion proteins, cultures of the transformed cells were separated into medium, cell wall, cellular membrane and cellular soluble fractions. Proteins in these fractions were separated, and the distribution of the GFP-fusion proteins was analyzed (Fig. 1C). GFP-AGP was recovered predominantly in the membrane fraction and to a lesser extent in the soluble fraction, and trace amounts were present in the cell walls and culture medium. In the case of GFP-AGPΔC, most of the large smear was recovered in the medium, and a small amount of this form was also found in the membrane and soluble fractions. In contrast, almost all the 48-kDa form was recovered in the membrane fraction and the smallest 37-kDa form was recovered in the soluble fraction. In the case of PIP-GFP, which was used as the fractionation control, most of this protein was recovered in the membrane fraction with a trace amount in the cell walls, and faint signals of smaller forms, possibly truncated ones, were detected in the soluble fraction.

We next addressed the distribution of the GFP fluorescence from 7-day-old cells expressing either GFP-AGP or GFP-AGPΔC by confocal laser scanning microscopy (CLSM) (Fig. 2). Almost all the green florescence in GFP-AGP-expressing cells was localized at the cell surface, possibly at the PM, and a very faint signal was observed in the vacuoles (Fig. 2A & B). In contrast, cells expressing GFP-AGPΔC showed weak green fluorescence in the vacuoles with an unidentified punctate structure with green fluorescence close to the cell wall (Fig. 2C & D). The latter punctate signal could have

bioRxiv preprint doi: https://doi.org/10.1101/2020.10.19.346049; this version posted October 19, 2020. The copyright holder for this preprint (which was not certified by peer review) is the author/funder. All rights reserved. No reuse allowed without permission.

been the autofluorescence of the cells, since a similar signal was also detected in non-transformed cells (Fig. 2E & F).

To determine whether the green fluorescence from GFP-AGP-expressing cells was localized to the PM, we observed the cells after plasmolysis (Fig. 2G). The clear line of a green fluorescence signal, which corresponded to a Hechtian strand, was visible between the PM and cell walls. This indicated that GFP-AGP was localized to the PM. To further confirm that the GFP-AGP signal was localized in the PM, the cells were incubated for 5 min with FM 4-64, and both the green and red fluorescence were recorded (Fig. 2H-J). The green and red fluorescence colocalized well, although the intensity of the green signal did not appear to be uniform. This observation also confirmed that GFP-AGP was localized to the PM. To assess the non-uniform localization of GFP-AGP at the PM, Z-stack images were collected by CLSM and then a 3D image was reconstituted (Supplemental movie 1). The non-uniform distribution of GFP fluorescence was apparent in the reconstituted 3D image. These data indicated that GFP-AGP was predominantly localized to the PM with non-uniform distribution.

Although these data suggested that NtAGP1 is a PM protein, we could not confirm this localization by the result of the expression of only one fusion protein, and also we found it difficult to further characterize GFP-AGP for several reasons. First, the green fluorescence from GFP-AGP was unstable in the stably-transformed tobacco BY-2 cells, and within six weeks of subculture, almost all the cells stopped emitting green fluorescence. Secondly, the signal peptide-GFP fusion protein was not fully secreted to the culture medium from tobacco BY-2 cells (Mitsuhashi et al., 2000). Thus, GFP alone may not be a good cargo for secretion, the flow path that may be the default pathway from the ER in the endomembrane transport system. Thirdly, we have a fluorescence pulse-chase system using a photo-convertible fluorescence protein, mKikGR (Habuchi et al., 2008) that have similar higher order structure with GFP, to monitor the turnover of proteins (Abiodun and Matsuoka, 2013). Therefore, we tried to apply this system to address the transport of NtAGP1 by expressing the fusion protein of mKikGR and NtAGP1 in tobacco BY-2 cells. Unfortunately, the fusion protein migrated with three distinct bands: a weak large smear that migrated at a position similar to GFP-AGP, a predominant band around 60 kDa, and a weaker band around 50 kDa (Supplemental Fig. 1). We therefore tested the transport and modification of NtAGP1 using a protein with structurally distinct from GFP as a tag to determine the localization and transport of this protein and its mutant lacking a GPI-anchoring signal.

bioRxiv preprint doi: https://doi.org/10.1101/2020.10.19.346049; this version posted October 19, 2020. The copyright holder for this preprint (which was not certified by peer review) is the author/funder. All rights reserved. No reuse allowed without permission.

Expression and localization of the sporamin-NtAGP1 fusion protein and its mutant lacking an GPI-anchoring signal in tobacco BY2-cells

We used sweet potato sporamin as another protein tag to address the transport, localization and modification of NtAGP1 and its derivative lacking a GPI-anchoring signal. Sporamin is a monomeric soluble and non-glycosylated storage protein of sweet potato (Maeshima et al., 1985) localized in the vacuoles (Hattori et al., 1988). Expression of a mutant precursor to sporamin, which does not contain the propeptide region but does contain the signal peptide for secretion in tobacco BY-2 cells, allowed the efficient secretion of this protein to the medium (>90% of this pulse-labeled protein is secreted within 2 h of chase) (Matsuoka and Nakamura, 1991). The junction region between the propeptide and the mature sporamin surrounding the 36th Pro residue consists of a cryptic Hyp O-glycosylation site for AG, and thus both a wild-type precursor to sporamin as well as mutant precursors with a disrupted vacuolar targeting signal are O-glycosylated when expressed in tobacco BY-2 cells (Matsuoka et al., 1995, Matsuoka and Nakamura, 1999). The efficiency of secretion of mutants with a disrupted vacuolar targeting signal is comparable to that of the mutant without the propeptide (Matsuoka and Nakamura, 1999). In other words, the secretion efficiency of sporamin is not affected by the presence or absence of O-glycosylation. We thus chose sporamin as another protein tag to analyze the transport and modification of NtAGP1 and its mutant lacking a GPI-anchoring signal.

The expression constructs for the signal peptide-sporamin-mature NtAGP1 with a GPI-anchoring signal (SPO-AGP) or those for the signal peptide-sporamin-mature NtAGP1 without a GPI-anchoring signal (SPO-AGPΔC) (Fig. 3A) were expressed in tobacco BY-2 cells. Cell and medium fractions were prepared from stationary-grown transformed BY-2 culture, and then the intra- and extra-cellular localizations of sporamin or its fusion proteins in these fractions were examined by immunoblotting either directly without immunoprecipitation (Fig. 3B) or after target proteins were recovered by immunoprecipitation (Fig. 3C). Immunoblotting without immunoprecipitation gave cross-reacted protein bands in proteins from non-transformed cells (Fig. 3B, WT). Such signals were absent after immunoprecipitation (Fig. 3C, WT). However, comparison of the intensities of sporamin-related signals on many immunoblots carried out under both these conditions indicated that the recovery by immunoprecipitation varied among the proteins, especially SPO-AGP. Thus, we did not use immunoprecipitation for the subsequent quantitative analysis, and always included a negative control from non-transformed cells.

bioRxiv preprint doi: https://doi.org/10.1101/2020.10.19.346049; this version posted October 19, 2020. The copyright holder for this preprint (which was not certified by peer review) is the author/funder. All rights reserved. No reuse allowed without permission.

SPO-AGP was detected as a smear band close to the top of the SDS-polyacrylamide gel (Figs. 3B, C). This observation indicated that SPO-AGP was glycosylated. Most of the smear-migrating protein was recovered in the cell fraction (Fig. 3B). On the other hand, SPO-AGPΔC was detected as three distinct species with different migration positions; a large form that migrated at the 90-120 kDa position, an intermediate form at the 36 kDa position and a small one at the 22 kDa position (Figs. 3B, C). A specific band that migrated at the front of electrophoresis gel may have been the degradation product of SPO (Figs. 3B). A large SPO-AGPΔC was detected in both the cell and medium fractions. Because the molecular weight of non-glycosylated SPO-AGPΔC is calculated as 27.5 kDa, this observation indicated that most of the large SPO-AGPΔC was glycosylated and secreted into the extracellular space. The intermediate and small SPO-AGPΔC were detected in cell fractions. This observation suggests that they were localized in the cells. The small form may be the degradation product, since its size (22 kDa) was similar to that of SPO (Fig. 3C) and smaller than the calculated size of the non-glycosylated form of SPO-AGPΔC.

To reveal the intracellular localization of SPO-AGP and SPO-AGPΔC, we performed subcellular fractionation by differential centrifugation. Cell lysates were centrifuged at 1,000*g* and the precipitate, defined as the P1 fraction, which contained unbroken cells, nuclei and cell walls, was collected. The supernatant was centrifuged at 10,000*g* and the precipitate (P10), which contained most of the mitochondria and plastids, was collected. The resulting supernatant was further centrifuged at 100,000*g* and the obtained precipitate (P100) contained microsomal membranes. The supernatant, which was defined as the S fraction, was also collected. SPO-AGP was detected in the P1, P100 and S fractions (Fig. 3D). In the case of SPO-AGPΔC, the large and small forms were detected in the P1 and S fractions, while the intermediate form was observed in all fractions (Fig. 3E).

To address the localization SPO-AGP, which was recovered in the P100 fraction, we prepared microsomal membranes from transformed BY-2 cells expressing SPO-AGP using buffers containing either $MgCl_2$ or EDTA, and then separated the membranes by equilibrium sucrose density gradient centrifugation in the presence or absence of Mg^{2+}, respectively. The distribution of SPO-AGP in these separated fractions was examined by immunoblotting (Fig. 4). The distributions of marker proteins were also analyzed by immunoblotting with specific antibodies: Sec61 for the ER (Yuasa et al., 2005), vacuolar pyrophosphatase (V-PPase) for tonoplast (Toyooka et al., 2009), GLMT1 for the Golgi apparatus (Liu et al., 2015), plasma membranous ATPase (P-ATPase) for PM (Toyooka et al., 2009) and PM water channel (PIP) for

bioRxiv preprint doi: https://doi.org/10.1101/2020.10.19.346049; this version posted October 19, 2020. The copyright holder for this preprint (which was not certified by peer review) is the author/funder. All rights reserved. No reuse allowed without permission.

PM (Suga et al., 2001). In the presence of Mg^{2+} (Fig. 4A), SPO-AGP migrated in several fractions, mainly in the fractions corresponding to 41-44(w/w)% sucrose. Quantification of the intensities of these immunoblot signals indicated that the migration pattern of SPO-AGP was similar to those of P-ATPase and PIP, the markers of the PM. In the absence of Mg^{2+} (Fig. 4B), SPO-AGP also migrated with a peak at around 41-43(w/w)% sucrose. This migration pattern was also similar to that of P-ATPase and PIP. These fractionation data indicated that SPO-AGP was localized to the PM.

Intracellular localization of SPO-AGPΔC

We prepared protoplasts from transformed BY-2 cells expressing SPO-AGPΔC in order to determine which forms of SPO-AGPΔC were localized outside of the PM (Fig. 5A). The large SPO-AGPΔC was detected only in cells and was not detected in protoplasts. The intermediate protein was detected in both cells and protoplasts, although the amount was smaller in protoplasts than in cells. The small SPO-AGPΔC was detected in both of these fractions in nearly equal amounts. This result indicated that the large SPO-AGPΔC was localized in the periplasm and cell wall, intermediate SPO-AGPΔC was localized in both the periplasm and the cells, and the small SPO-AGPΔC was localized almost exclusively in the cells.

To address whether some of the intracellular SPO-AGPΔC was localized in vacuoles, we separated protoplasts into vacuoplast and cytoplast fractions and analyzed the amounts of the different forms of SPO-AGPΔC in these fractions. The vacuoplasts are composed of vacuoles surrounded with the PM, and cytoplasts are composed of cytoplasm, nuclei and PM. We measured the protein concentration in the protoplast and cytoplast fractions, and α-mannosidase activity in the protoplast and vacuoplast fractions. Thereafter, proteins that were present in the protoplast and cytoplast fractions in nearly equal amounts, and proteins that were present in protoplast and vacuoplast fractions in amounts almost equivalent to the levels of f α-mannosidase activity were separated by SDS-PAGE, and the different forms of SPO-AGPΔC in these fractions were detected by immunoblotting (Fig. 5B). Mitochondrial porin was used as a fractionation control. The intermediate SPO-AGPΔC was detected in the protoplast and cytoplast fractions in nearly equal amounts relative to the protein, whereas the small form was detected in both the protoplast and vacuoplast fractions in amounts similar to the activity of α-mannosidase. This result suggests that the small SPO-AGPΔC was localized in vacuoles and the intermediate SPO-AGPΔC was localized in other intracellular compartments.

bioRxiv preprint doi: https://doi.org/10.1101/2020.10.19.346049; this version posted October 19, 2020. The copyright holder for this preprint (which was not certified by peer review) is the author/funder. All rights reserved. No reuse allowed without permission.

To investigate the localization of the intermediate SPO-AGPΔC in cells, we prepared microsomal fractions from transformed BY-2 cells expressing SPO-AGPΔC in buffers containing either $MgCl_2$ or EDTA. The microsomal membranes were separated by equilibrium sucrose density gradient centrifugation in the presence or absence of Mg^{2+}, respectively. The distribution of the intermediate SPO-AGPΔC in these separated fractions was examined by immunoblotting and compared to the distributions of marker proteins in the secretory organelles (Fig. 5C, D). In the presence of Mg^{2+} (Fig. 5C), the intermediate SPO-AGPΔC migrated in several fractions with a peak at around 39-42 (w/w)% sucrose. This migration pattern was similar to that of Sec61, a marker of the ER membrane. In the absence of Mg^{2+} (Fig. 5D), the intermediate SPO-AGPΔC also migrated with a peak at around 31-34(w/w)% sucrose, and the peak shifted to a lower-density position compared with that in the presence of Mg^{2+}. This shift corresponded to that of the migration pattern of Sec61 (ER marker). These fractions did not contain P-ATPase and PIP but did contain GLMT1, the marker of the Golgi apparatus. These fractionation data suggest that the intermediate SPO-AGPΔC is localized predominantly in the ER and partly in the Golgi apparatus.

NtAGP1 is a GPI-anchored protein

The NtAGP1 precursor contains a GPI-anchoring signal at its C-terminus. We showed that GFP-AGP and SPO-AGP were localized to the PM (Figs. 2 and 5). To determine whether the GPI-anchoring signal on the NtAGP1 precursor is functional and whether the GPI-anchor attached to NtAGP was responsible for attaching this protein to the PM, we analyzed the distribution of these fusion proteins recovered in the microsomal fraction by two-phase separation using Triton X-114. A nonionic detergent such as Triton X-114 can be used to make a uniform solution at low temperature, which can then be separated into two phases, such as an aqueous (aqu) phase and a detergent-rich (det) phase, at higher temperature. By taking advantage of this characteristic of the nonionic detergent, a cell extract can be separated into soluble and peripheral membrane proteins that can be recovered in the aqu phase, and integral membrane proteins as well as lipid-anchored proteins that can be recovered in the det phase (Bordier, 1981).

Around half of the GFP-AGP (Fig. 6A, left), as well as almost all of the SPO-AGP (Fig. 6B, top left) and almost all of the PIP-GFP (an integral membrane protein used as an experimental control; Fig. 6A, right), was recovered in the det fraction. Under the same separation condition, almost all the smear-migrating GFP-AGPΔC and

bioRxiv preprint doi: https://doi.org/10.1101/2020.10.19.346049; this version posted October 19, 2020. The copyright holder for this preprint (which was not certified by peer review) is the author/funder. All rights reserved. No reuse allowed without permission.

SPO-AGPΔC were recovered in the aqu fraction. These observations suggested that around half of the GFP-AGP and almost all of the SPO-AGP were localized to the PM with their GPI-anchors. To address whether this membrane-association is actually mediated by the GPI-anchor attached to these proteins, two-phase separation experiments were carried out in the presence of phosphatidylinositol-specific phospholipase C (PI-PLC), which can cleave the phosphodiester bond in a GPI-anchor (reviewed by Hopper, 2001). In the presence of PI-PLC, almost all the GFP-AGP in the microsomal fraction was recovered in the aqu phase (Fig. 6C, right). Likewise, around half of the SPO-AGP that was recovered in the TX-114 phase was recovered in the det phase (Fig. 6D, top). Under the same condition, vacuolar pyrophosphatase, which is an integral membrane protein used as a control, was recovered almost exclusively in the det phase (Fig. 6D, bottom). These observations indicated that roughly half of both GFP-AGP and SPO-AGP was anchored to the PM by a GPI-anchor that was sensitive to PI-PLC and suggested that NtAGP1 is a GPI-anchored protein at the PM.

GPI-anchoring is required for the proper assembly of AGP glcyan

We showed that the migration position of the smear-migrating SPO-AGP and SPO-AGPΔC on SDS-polyacrylamide gel were different (Fig. 3A, B). We considered that this difference might be due to the difference in AG glycan chains on these proteins. To address this possibility, we examined the reactivity of anti-AG glycan monoclonal antibodies (mABs) to these proteins. Among the mABs that we tested, SPO-AGPΔC was specifically recognized by LM2 (Fig. 7B). In addition, both proteins were recognized by LM6 (Fig. 7C). Other antibodies, namely PN16.4B4, CCRC-M7, MAC204, and MAC207, did not recognize both proteins. Because LM2 recognizes terminal β-glucuronic acid (β-GlcA) (Yates et al., 1996), the absence of recognition of SPO-AGP by this antibody indicated that such a structure was absent in the glycan in SPO-AGP. This result also suggested that GPI-anchoring is required for the proper assembly of AGP glycan.

Discussion

In this work we investigated the role of the GPI-anchor on the transport and modification of NtAGP1, a classical AGP in tobacco. The expression of the GFP fusion protein in tobacco BY-2 cells allowed us to detect the smear-migrating GFP-fusion protein with low mobility on SDS-polyacrylamide gel (Fig. 1). This behavior of the fusion protein was consistent with the typical migration pattern of AGP

bioRxiv preprint doi: https://doi.org/10.1101/2020.10.19.346049; this version posted October 19, 2020. The copyright holder for this preprint (which was not certified by peer review) is the author/funder. All rights reserved. No reuse allowed without permission.

in many plant species (e.g., Putoczki et al., 2007; Yang and Showalter, 2007; Lind et al., 1994; Maurer et al., 2010). In contrast, the fusion protein formed using another fluorescent protein, mKikGR (Habuchi et al., 2008), yielded one slow-migrating and two fast-migrating smear bands (Supplemental fig. 1). To determine which of the observed migration behaviors of these fusion proteins represented the true nature of NtAGP1, we characterized another fusion protein formed with sporamin and found that this fusion protein migrated as a slow-migration smear band on SDS-polyacrylamide gel (Fig. 3). We therefore concluded that the slow migration and formation of a smear band on SDS-polyacrylamide gel are characteristic of NtAGP1. These observations also suggested that differences in the non-glycosylated region of AGP may affect the degree of modification of the protein.

Analyses of the localization of GFP-AGP and SPO-AGP indicated that most of these proteins were localized to the PM (Figs. 2A, G, H and Fig. 4), and that both proteins were attached to the PM as GPI-anchored forms (Fig. 6). In addition, some of these proteins were recovered in the medium and were also present in the periplasmic space. These observations suggested that NtAGP1 is a GPI-anchored PM protein, although some NtAGP1 is also released to the extracellular space following cleavage of its GPI-anchor, possibly via the actions of phospholipase in the extracellular space.

In contrast to the fusion proteins with an intact AGP with GPI-anchoring signal, mutant fusion proteins without a GPI-anchoring signal—namely, GFP-AGPΔC and SPO-AGPΔC—were detected as multiple bands at different migration positions on SDS-polyacrylamide gels (Figs. 1 and 3). The glycosylated forms of these proteins that migrated the most slowly and most readily formed smear bands were predominantly recovered in the medium fraction (Figs. 1 and 3). Fractionation analysis of cells expressing these proteins indicated that the intermediate forms were recovered partly in the membranous organelles in the cells and partly in the periplasmic space (Figs. 1 and 3). The migration positions of these proteins on SDS-polyacrylamide gels were slower than those of the calculated size of non-glycosylated forms of these proteins, suggesting that these proteins are modified to some extent, probably with glycans. Purification of these proteins and analysis of their sugar compositions will clarify whether such modification takes place.

The fractionation study of microsomes from SPO-AGPΔC-expressing cells indicated that the intermediate SPO-AGPΔC was localized in the ER with partial localization in the Golgi (Fig. 5). The smallest forms of this protein, which was similar in size to SPO, was recovered in the soluble fraction from the cells, which consisted of the cytoplasm and vacuolar sap. The smallest form of SPO-AGPΔC was also recovered

bioRxiv preprint doi: https://doi.org/10.1101/2020.10.19.346049; this version posted October 19, 2020. The copyright holder for this preprint (which was not certified by peer review) is the author/funder. All rights reserved. No reuse allowed without permission.

in the vacuoplast fraction. These observations indicated that some of the SPO-AGPΔC protein was transported to the vacuoles, while most of the AGP part of these proteins was cleaved off or degraded in the vacuoles.

These observations indicated that GPI-anchoring is not only essential for the proper and efficient transport of NtAGP1 to the plasma membrane or extracellular space but also required for the efficient glycosylation. Some of the inefficient-modified forms, the intermediate forms, were retained in the ER, and some of them could also be transported to the vacuoles for degradation. These observations were partly consistent with the case of a Citrin-tagged and GPI-anchoring signal-deleted fasciclin-like AGP mutant (Xue et al., 2017). In this case, most of the mutant protein was retained in the ER. In our present experiments, however, vacuolar localization was observed. This difference in vacuolar localization between the previous report and our present study might be attributable to either the different detection systems or different proteins used.

It has been reported that the vacuoles are scavenger organelles that degrade damaged proteins and organelles. In yeast, it has been shown that vacuolar targeting is a mechanism for degrading improperly folded proteins in the ER, and this transport is mediated by a receptor for vacuolar targeting (Hong et al., 1996). In plants, targeting of soluble proteins to the lytic vacuoles (such as the central vacuoles in tobacco BY-2 cells) is mediated by VSR proteins (reviewed in Shimada et al., 2018). Large and hydrophobic residues, such as Ile and Leu, in the vacuolar-sorting determinants in proteins play a pivotal role in the targeting (Ahmed et al., 2000; Brown et al., 2003; Matsuoka and Nakamura, 1995, 1999; Paris et al., 1997). Therefore, it is interesting that inefficient glycosylation of SPO-AGPΔC may cause the exposure of a large and hydrophobic side chain in the mature region of AGP, and this characteristic of SPO-AGPΔC may have allowed the targeting of this protein to the vacuole after recognition by VSR proteins, as in the case of yeast (Hong et al., 1986). In fact, the SPLA sequence at amino acid positions 67 to 70 of the NtAGP1 precursor resembles the NPIR vacuolar sorting determinants of sporamin and aleurain propeptides (Matsuoka and Nakamura, 1995, 1999; Paris et al., 1997), and this region may be a good candidate for a region that is exposed under inefficient glycosylation.

Not only the mislocalization but also alteration of the glycan moiety was observed in the secreted SPO-AGPΔC from SPO-AGP (Fig. 7). Secreted SPO-AGPΔC was recognized by the mAB LM2, which was previously shown to recognize β-glucuronic acid (β-GlcA) residues in AG glycan (Yates et al., 1996). Competition analysis suggested that further modification to the β-GlcA moiety abolished the binding (Yates et al., 1996). It has been shown that the structure of the glycan moiety of artificial AGP

bioRxiv preprint doi: https://doi.org/10.1101/2020.10.19.346049; this version posted October 19, 2020. The copyright holder for this preprint (which was not certified by peer review) is the author/funder. All rights reserved. No reuse allowed without permission.

475 secreted from tobacco BY-2 cells contains β-GlcA, which is further modified partly by
476 rhamnose (Tan et al., 2004, 2010). In addition, the β-GlcA moiety of AGP is
477 sometimes methylated by the action of DUF576 family methyltransferases (Temple et
478 al., 2019). Thus, it is possible that the glycan structure of secreted SPO-AGPΔC is
479 similar to that of the artificial AGPs, which contain a terminal β-GlcA, whereas such a
480 structure is absent in SPO-AGP, and that this difference is achieved by an efficient
481 modification with rhamnose or methyl residues. Future analysis of the sugar
482 compositions of the purified SPO-AGP and secreted SPO-AGPΔC proteins will be
483 needed to fully explore these possibilities.
484 What causes the difference in glycan structure between SPO-AGP and secreted
485 SPO-AGPΔC? One possible answer may be related to the difference in transport routes
486 of these proteins in the late secretory pathway, with different distributions of the
487 enzymes responsible for modification for the AGP glycan. It was shown in tobacco
488 protoplasts using a GFP-tagged pectin methylesterase inhibitor protein and its mutant
489 without a GPI-anchoring signal that the late transport pathways of these proteins are
490 different (De Caroli et al., 2011). The DUF576 family methyltransferases that act
491 against AGP glycan have been detected not only in the Golgi apparatus but also in
492 small punctate structures that are distinct from the Golgi apparatus (Temple et al.,
493 2019). Similarly, a subset of glycosyltransferases involved in AGP glycan biogenesis
494 was found in a non-Golgi punctate structure with an exocyst protein Exo70 homolog 2,
495 which is a marker for exocyst-positive organelles, but not with a SNARE protein
496 SYP61, which is localized in the *trans*-Golgi network (TGN) and subsequent secretory
497 vesicles (Poulsen et al., 2015). Recent analysis of the secretome of *Arabidopsis*
498 indicated that there are at least two distinct secretory pathways in *Arabidopsis* leaf
499 cells (Uemura et al., 2019). One of these pathways, which depends on SYP4-type
500 SNAREs, is involved in the secretion of many hydrolases (Uemura et al., 2019). In an
501 analysis focusing on AGP in the data generated and describe in this paper (PRIDE
502 dataset identifier PXD009099 by H. Nakagami and co-workers), only a small fraction
503 of AGPs with GPI-anchoring signal (18%) showed significantly high abundance in
504 apoplasts in a wild-type relative to a mutant with SYP4-type SNARE proteins
505 (Supplemental table 1). In contrast, when the same approach was taken against two
506 groups of secretory hydrolases, namely, pectic-lyase like proteins without a
507 GPI-anchoring signal and β-galactosidase, a greater proportion of these proteins
508 showed a high level of secretion in the wild-type than the mutant SYP4-type SNARE
509 proteins (35% and 38%, respectively). In *Arabidopsis*, the SYP4-type SNAREs are
510 localized in not only TGN adjusting the Golgi apparatus but also a small punctate

bioRxiv preprint doi: https://doi.org/10.1101/2020.10.19.346049; this version posted October 19, 2020. The copyright holder for this preprint (which was not certified by peer review) is the author/funder. All rights reserved. No reuse allowed without permission.

structure that is called the Golgi-independent TGN or free TGN (Viotti et al., 2010; Kang et al., 2011; Uemura et al., 2014). A similar structure called a secretory vesicle cluster (SVC), which is involved in pectin secretion, is found in tobacco BY-2 cells (Toyooka et al., 2009). Analysis of the proteome and glycome of secretory vesicles marked with SYP61 indicated that these secretory vesicles are rich in the SYP4-type SNARE proteins as well as glycans that are recognized by mABs against pectin (Drakakaki et al., 2012; Wilkop et al., 2019). Although glycans in the same vesicle fraction are also recognized by mABs against AGP, this recognition is weaker than that in the cell wall fraction, in contrast to the recognition by mABs that recognize pectin (Fig. 3 in Wilkop et al., 2019). Collectively, these observations suggest that the GPI-anchored AGP precursor is predominantly transported from TGN to an exocyst-positive organelle, where a subset of glycosyltransferases and/or methyltransferases localize, and then is transported to the PM after efficient modification of the glycan in the compartment. The absence of a GPI-anchor in the AGP precursor prevents to take this route from TGN and passes through the default secretion pathway, and this mis-sorting limits the final maturation of AGP glycan.

Another possible explanation for the difference in glycan structure is that the accessibility to the modification enzymes might not be efficient in the absence of a GPI-anchor. Because most of the glycosyltransferases and methyltransferases in the secretory pathway are integral membrane proteins whose catalytic domains are located proximately to the phospholipid bilayer, the GPI-anchoring of the AGP precursor will bring the protein close to the catalytic sites of these enzymes. Without a GPI-anchor, such access would not be efficient, and this characteristic would prevent efficient maturation of the glycan side chain. The third possibility is that the transport speed is different between SPO-AGP and SPO-AGPΔC, and this difference contributes to the difference in the glycan side chain. Future studies to address the pathways and kinetics of transport and modification of AGP using SPO-AGP as a model will reveal which scenario or combination of scenarios is most likely.

Conclusion

The fusion protein of GFP or SPO and NtAGP1 expressed in BY-2 cells migrated as a large smear on SDS-polyacrylamide gel and localized to the plasma membrane as a GPI-anchored form. In contrast, the expression of mutants without a GPI-anchoring signal yielded several forms, and the largest forms with large smears were secreted into the culture medium, whereas other forms were recovered in the endomembrane organelles. Comparison of the glycan structure of SPO-AGP recovered in microsomes

bioRxiv preprint doi: https://doi.org/10.1101/2020.10.19.346049; this version posted October 19, 2020. The copyright holder for this preprint (which was not certified by peer review) is the author/funder. All rights reserved. No reuse allowed without permission.

and secreted mutant SPO-AGP without a GPI-anchoring signal using antibodies against AGP glycan epitopes indicated that the glycan structures of these proteins are different. Therefore, the GPI-anchoring signal is required for both the proper transport and proper glycosylation of the AGP precursor.

Materials and Methods

Construction of plasmid

The pilot 5'-sequence of clones from the EST of tobacco BY-2 cells (Galis et al., 2006) allowed the identification of a clone (BY28237, GeneBank accession No. LC128049.1) encoding the NtAGP1 protein (GeneBank accession No. BAU61512), which is a typical AGP precursor nearly identical to a *Nicotiana alata* AGP precursor (Du et al., 1994). The signal peptide and GPI-anchoring signal were predicted using SignalP (http://www.cbs.dtu.dk/services/SignalP-3.0/) and PredGPI (http://gpcr.biocomp.unibo.it/predgpi/), respectively. Using this information and the PCR primers in Supplemental table 2, the expression constructs used in this study were generated. The fusion protein of GFP and NtAGP1, designated as GFP-AGP, was designed as follows. The signal peptide and two amino acids from the cleavage site of the signal peptide were linked to a mutant GFP (sGFP(S65T); Chiu et al., 1996), and then the C-terminus of this GFP was linked to the mature part and the GPI-anchoring signal of NtAGP1 by joining PCR. Using the EST as a template and primers P1 and P2, the coding region for the signal peptide and two amino acids with the N-terminal region of the GFP coding sequence was amplified. Using a sGFP(S65T)-containing plasmid (Shimizu et al., 2005) as a template and primers P3 and P4, a DNA fragment encoding part of a signal peptide, two amino acids of mature NtAGP1, GFP and the N-terminal part of mature NtAGP1 was amplified. Using the EST as a template and primers P5 and P6, a fragment encoding the C-terminal amino acids of GFP fused with the mature NtAGP1 and GPI-anchoring signal was amplified. After mixing these three fragments, the fusion construct was amplified using P1 and P6 primers. After digesting the resulting fragment with BglII and EcoRI restriction enzymes, because the primers also contain sequences for these enzymes, the fragment was cloned into the corresponding sites of plant expression vector pMAT137 (Yuasa et al., 2004). Using this plasmid as a template and primers P1 and P7, a fragment encoding GFP-AGPΔC was amplified. The resulting fragment was digested with BglII and EcoRI and cloned into pMAT137 as described above.

bioRxiv preprint doi: https://doi.org/10.1101/2020.10.19.346049; this version posted October 19, 2020. The copyright holder for this preprint (which was not certified by peer review) is the author/funder. All rights reserved. No reuse allowed without permission.

For the construction of sporamin fusions, the coding sequence for the signal peptide and mature sporamin fusion construct (Δpro sporamin; Matsuoka and Nakamura, 1991) was used for the signal peptide-sporamin region. Using P8 and P9 as primers and a plasmid with the Δpro sporamin construct (pMAT108: Matsuoka and Nakamura, 1991) as a template, the region for signal peptide-sporamin with the N-terminal region of mature NtAGP1 was amplified. Using the GFP-AGP-expressing plasmid described above as a template and primers P10 and P11, a fragment encoding the C-terminal region of sporamin with mature AGP and a GPI-anchoring signal was amplified. After mixing these amplified fragments and primers P8 and P11, a fragment encoding the SPO-AGP fusion protein was amplified. The resulting fragment was digested with BglII and EcoRI and cloned into pMAT137 as described above. Using this plasmid as a template and primers P8 and P12, a fragment encoding SPO-AGPΔC was amplified. The resulted fragment was digested with BglII and EcoRI and cloned into pMAT137 as described above.

Culture and transformation of tobacco BY-2 cells

The plant expression plasmids generated for the expression of AGP fusion proteins were then used to transform tobacco BY-2 cells with *Agrobacterium* as described previously (Matsuoka and Nakamura, 1991). Cultures of tobacco BY-2 cells and their transformants were maintained as described previously (Matsuoka and Nakamura, 1991). Seven-day-old cells (stationary phase) were used in all the experiments except when stated otherwise in the figure legends.

Confocal microscopy and image analysis

The localizations of GFP-AGP and GFP-AGPΔC expressed in transformed BY-2 cells were visualized using a Leica TCS SP8 confocal laser scanning microscope as described previously (Tasaki et al., 2014). In some cases, Z-stack images were collected and converted to a rotating movie. To visualize the plasma membrane using FM 4-64, cells were stained with FM 4-64 for 5 to 10 min as previously described for FM1-43 (Emans et al., 2002). Confocal images of the red fluorescence of stained cells were collected as described previously (Tasaki et al., 2014).

Antibodies

A recombinant protein corresponding to the 14^{th} to 165^{th} positions of tobacco mitochondrial porin, encoded by the tobacco EST clone BY5432 (Gene Bank BP133193; Matsuoka et al., 2004) was expressed as a T7- and His_6- tagged protein in

bioRxiv preprint doi: https://doi.org/10.1101/2020.10.19.346049; this version posted October 19, 2020. The copyright holder for this preprint (which was not certified by peer review) is the author/funder. All rights reserved. No reuse allowed without permission.

E. coli after subcloning the corresponding fragment into a pET23 expression vector. The recombinant protein was purified using the His_6-tag and used as an antigen to immunize a Japanese white rabbit. Antiserum from this rabbit was then used as anti-mitochondrial porin. Antisera against SDS-denatured SPO (Matsuoka and Nakamura., 1991), affinity purified anti-plant Sec61 (Yuasa et al., 2005), anti V-PPase (Toyooka et al., 2009), anti-PIP (Suga et al., 2001), and anti-GLMT1 (Liu et al., 2015) antibodies were used at the appropriate dilutions. Monoclonal anti-AGP glycan antibodies, LM2 and LM6 (Yates et al., 1996), were purchased from PlantProbes. To visualize the antigen-antibody complex by immunoblotting, Alexa Flour 568 goat anti-rabbit IgG (H+L), Alexa Flour 568 goat anti-mouse IgG (H+L), Alexa flour 647 goat anti-rat IgG (H+L) or Alexa Flour 647 goat anti-rat IgM (μ chain) was purchased from Invitrogen (Eugene, OR) and used as a secondary antibody.

SDS-PAGE and detection of fusion proteins

To estimate the size and extent of modification of the fluorescent fusion proteins, the proteins were separated by SDS-PAGE, and their fluorescence was recorded by direct scanning of the gel using a Typhoon 9600 image analyzer (GE Healthcare Bio-Science, Chicago, IL) as described previously (Tasaki et al., 2014). For the detection of SPO fusion proteins and AGP glycan, immunoblotting was carried out as described previously (Oda et al., 2020) using an appropriate primary and fluorescence-tagged secondary antibodies.

For the comparison of the reactivities of SPO-AGP and secreted SPO-AGPΔC against anti-glycan antibodies, Adjustment of the loading of SPO-AGP in the microsomes and secreted large form of SPO-AGPΔC was carried out after semi-quantitative immunoblotting using various amounts of microsomes from SPO-AGP-expressing cells and medium from SPO-AGPΔC culture. Thereafter the volumes of the microsomes and the medium that gave nearly identical intensity when detected using an anti-sporamin antibody were determined.

Immunoprecipitation

Immobilized anti-native sporamin was prepared as described previously (Matsuoka et al., 1995). Immunoprecipitation was performed essentially as described by Matsuoka and Nakamura (1991), except that the immobilized antibody was used instead of the anti-sporamin serum and protein A Sepharose.

Subcellular fractionation by differential centrifugation

bioRxiv preprint doi: https://doi.org/10.1101/2020.10.19.346049; this version posted October 19, 2020. The copyright holder for this preprint (which was not certified by peer review) is the author/funder. All rights reserved. No reuse allowed without permission.

Cells and media were separated from the suspension culture by filtration. A 10 g aliquot of the cells was mixed with 10 mL of buffer containing 0.45 M sucrose, 50 mM Tris-MES (pH 7.3), 2 mM DTT, 1(w/v)% Na-ascorbate, and a piece of cOmplete Mini EDTA-free (Roche, Basel, Switzerland), and disrupted by high-pressure N_2 using a Parr Cell Disruption Bomb MODEL4636 (Parr Instrument, Moline, IL) under 500 psi for 20 min. The disrupted suspension was centrifuged at 1,000 g for 10 min at 4°C and the supernatant was used as a total cellular fraction. For the differential centrifugation study, the supernatant was centrifuged at 10,000*g* for 10 min at 4°C. Next, the supernatant was centrifuged at 100,000*g* for 1 h at 4°C, then collected and supplemented with 1 x TBS up to 1 mL as a soluble fraction. The precipitates after the 1,000*g*, 10,000*g* and 100,000*g* centrifugations were resuspended with an equal volume of sonication buffer containing 1 x TBS (25 mM Tris-HCl (pH 7.4), 0.15 M NaCl), 1 mM EDTA, 1% Na-ascorbate, 100 μM Leupeptin, 1 mM PMSF / 0.5% isopropanol and 1 mM NEM and sonicated using a Bioruptor (COSMO BIO, Tokyo); the sonication condition consisted of power M at intervals of 0.5 min for 8 min. These sonicated suspensions were filled with 1 x TBS to a final volume of 1 mL and used as the P1, P10 and P100 fractions, respectively. These fractions were used for immunoprecipitation and analyzed by immunoblotting.

Preparation of microsomal fractions and fractionation using sucrose density gradient centrifugation

The preparation of microsomal fractions and fractionation of microsomes using linear sucrose density gradient centrifugation was performed essentially as described by Matsuoka et al. (1997), except that a Beckman SW28.1 rotor was used. The continuous gradient was centrifuged at 100,000 g for 18 h at 4°C. After centrifugation, 1 mL fractions were collected from the bottom to the top of the gradient.

Preparation of the protoplasts, vacuoplasts and cytoplasts

Protoplasts were prepared from transformed BY-2 cells as described by Nagata et al. (1981). Vacuoplasts and cytoplasts were prepared from protoplasts as described by Sonobe (1990).

Fractionation of GPI-anchored proteins by two-phase separation using Triton X-114

Precondensation of Triton X-114 and the fractionation of GPI-anchored proteins were performed as described by Murata et al. (2012) with the following modifications. One hundred microliters of the microsomal fraction was gently mixed with 380 μL of 1 x

bioRxiv preprint doi: https://doi.org/10.1101/2020.10.19.346049; this version posted October 19, 2020. The copyright holder for this preprint (which was not certified by peer review) is the author/funder. All rights reserved. No reuse allowed without permission.

TBS and 120 μL of ice-chilled precondensed Triton X-114, and incubated at 4°C overnight. The sample was centrifuged at 17,360*g* for 25 min at 4°C to remove detergent-insoluble materials. The supernatant was incubated at 37°C for 1.5 h and centrifuged at 13,000*g* for 5 min at room temperature to induce phase separation. The upper phase (aqueous phase) and the lower phase were collected. The lower phase was gently mixed with 400 μL of chilled 1 x TBS, then the phase separation procedure was repeated and the upper phase in this second-round separation was combined with the first upper phase and used as an aqueous phase fraction. The resulting detergent-rich phase was mixed with a 4-fold volume of ice-cold acetone and incubated at -20°C overnight. The proteins were recovered by centrifugation at 13,000*g* for 30 min at 4°C and the precipitate was collected and air-dried on ice. The precipitate was resuspended with 400 μL of 25 mM Tris-HCl (pH 7.4) and used as the det fraction. In some cases, 6.5 m units of PI-PLC (phospholipase C, phosphatidylinositol-specific from *Bacillus cereus*) (Sigma Aldrich, St. Louis, MO) were included during the incubation. For the processing of SPO-AGP, 200 μL of the det fraction was incubated with 1.8 m units of phospholipase C at 37°C for 2 h, and thereafter the two-phase separation with Triton X-114 was conducted.

Enzymes and protein assays

α-mannosidase activity was measured as described previously (Boller and Kende, 1979) using *p*-nitrophenyl phosphate as a substrate. Protein levels were measured using a DC protein assay kit (Bio-Rad).

Accession number

NtAGP1 cDNA sequence: LC128049.

Acknowledgments

We thank Dr. Koji Yuasa in RIKEN Plant Science Center for the production of recombinant mitochondrial porin and Mr. Nweke A. Boniface for improving the manuscript.

Literature Cited

bioRxiv preprint doi: https://doi.org/10.1101/2020.10.19.346049; this version posted October 19, 2020. The copyright holder for this preprint (which was not certified by peer review) is the author/funder. All rights reserved. No reuse allowed without permission.

Abiodun MO, Matsuoka K (2013) Evidence that proliferation of Golgi apparatus depends on both de novo generation from the endoplasmic reticulum and formation from pre-existing stacks during the growth of tobacco BY-2 cells. Plant Cell Physiol 54: 541-554

Basu D, Liang Y, Liu X, Himmeldirk K, Faik A, Kieliszewski M, Held M, Showalter AM (2013) Functional identification of a hydroxyproline-O-galactosyltransferase specific for arabinogalactan protein biosynthesis in Arabidopsis. J Biol Chem 288: 10132-10143

Basu D, Wang W, Ma S, DeBrosse T, Poirier E, Emch K, Soukup E, Tian L, Showalter AM (2015) Two hydroxyproline galactosyltransferases, GALT5 and GALT2, function in arabinogalactan-protein glycosylation, growth and development in Arabidopsis. PLoS One 10: e0125624

Boller T, Kende H (1979) Hydrolytic enzymes in the central vacuole of plant cells. Plant Physiol 63: 1123-1132

Bordier C (1981) Phase separation of integral membrane proteins in Triton X-114 solution. J Biol Chem 256: 1604-1607

Chiu W, Niwa Y, Zeng W, Hirano T, Kobayashi H, Sheen J (1996) Engineered GFP as a vital reporter in plants. Curr Biol 6: 325-330

De Caroli M, Lenucci MS, Di Sansebastiano GP, Dalessandro G, De Lorenzo G, Piro G (2011) Protein trafficking to the cell wall occurs through mechanisms distinguishable from default sorting in tobacco. Plant J 65: 295-308

Dilokpimol A, Poulsen CP, Vereb G, Kaneko S, Schulz A, Geshi N (2014) Galactosyltransferases from Arabidopsis thaliana in the biosynthesis of type II arabinogalactan: molecular interaction enhances enzyme activity. BMC Plant Biol 14: 90

Drakakaki G, van de Ven W, Pan S, Miao Y, Wang J, Keinath NF, Weatherly B, Jiang L, Schumacher K, Hicks G, Raikhel N (2012) Isolation and proteomic analysis of the SYP61 compartment reveal its role in exocytic trafficking in Arabidopsis. Cell Res 22: 413-424

Du H, Simpson RJ, Moritz RL, Clarke AE, Bacic A (1994) Isolation of the protein backbone of an arabinogalactan-protein from the styles of *Nicotiana alata* and characterization of a corresponding cDNA. Plant Cell 6: 1643-1653

Emans N, Zimmermann S, Fischer R (2002) Uptake of a fluorescent marker in plant cells is sensitive to brefeldin A and wortmannin. Plant Cell 14: 71-86

bioRxiv preprint doi: https://doi.org/10.1101/2020.10.19.346049; this version posted October 19, 2020. The copyright holder for this preprint (which was not certified by peer review) is the author/funder. All rights reserved. No reuse allowed without permission.

759 Gális I, Simek P, Narisawa T, Sasaki M, Horiguchi T, Fukuda H, Matsuoka K (2006) A
760 novel R2R3 MYB transcription factor NtMYBJS1 is a methyl
761 jasmonate-dependent regulator of phenylpropanoid-conjugate biosynthesis in
762 tobacco. Plant J 46: 573-592
763 Habuchi S, Tsutsui H, Kochaniak AB, Miyawaki A, van Oijen AM (2008) mKikGR, a
764 monomeric photoswitchable fluorescent protein. PLoS One 3: e3944
765 Hong E, Davidson AR, Kaiser CA (1996) A pathway for targeting soluble misfolded
766 proteins to the yeast vacuole. J Cell Biol 135: 623-633
767 Hooper NM (2001) Determination of glycosyl-phosphatidylinositol membrane protein
768 anchorage. Proteomics 1: 748-755
769 Kang BH, Nielsen E, Preuss ML, Mastronarde D, Staehelin LA (2011) Electron
770 tomography of RabA4b- and PI-4Kβ1-labeled *trans* Golgi network
771 compartments in Arabidopsis. Traffic 12: 313-329
772 Knoch E, Dilokpimol A, Tryfona T, Poulsen CP, Xiong G, Harholt J, Petersen BL,
773 Ulvskov P, Hadi MZ, Kotake T, Tsumuraya Y, Pauly M, Dupree P, Geshi N
774 (2013) A β-glucuronosyltransferase from Arabidopsis thaliana involved in
775 biosynthesis of type II arabinogalactan has a role in cell elongation during
776 seedling growth. Plant J 76: 1016-1029
777 Lind JL, Bacic A, Clarke AE, Anderson MA (1994) A style-specific
778 hydroxyproline-rich glycoprotein with properties of both extensins and
779 arabinogalactan proteins. Plant J 6: 491-502
780 Liu J, Hayashi K, Matsuoka K (2015) Membrane topology of Golgi-localized probable
781 S-adenosylmethionine-dependent methyltransferase in tobacco (Nicotiana
782 tabacum) BY-2 cells. Biosci Biotechnol Biochem 79: 2007-2013
783 Liu YS, Fujita M (2020) Mammalian GPI-anchor modifications and the enzymes
784 involved. Biochem Soc Trans 48: 1129-1138
785 Matsuoka K, Demura T, Galis I, Horiguchi T, Sasaki M, Tashiro G, Fukuda H (2004) A
786 comprehensive gene expression analysis toward the understanding of growth
787 and differentiation of tobacco BY-2 cells. Plant and Cell Physiology 45:
788 1280-1289
789 Matsuoka K, Higuchi T, Maeshima M, Nakamura K (1997) A Vacuolar-Type
790 H+-ATPase in a nonvacuolar organelle is required for the sorting of soluble
791 vacuolar protein precursors in tobacco cells. Plant Cell 9: 533-546
792 Matsuoka K, Nakamura K (1991) Propeptide of a precursor to a plant vacuolar protein
793 required for vacuolar targeting. Proc Natl Acad Sci U S A 88: 834-838

bioRxiv preprint doi: https://doi.org/10.1101/2020.10.19.346049; this version posted October 19, 2020. The copyright holder for this preprint (which was not certified by peer review) is the author/funder. All rights reserved. No reuse allowed without permission.

794 Matsuoka K, Nakamura K (1999) Large alkyl side-chains of isoleucine and leucine in
795 the NPIRL region constitute the core of the vacuolar sorting determinant of
796 sporamin precursor. Plant Mol Biol 41: 825-835
797 Matsuoka K, Watanabe N, Nakamura K (1995) O-glycosylation of a precursor to a
798 sweet potato vacuolar protein, sporamin, expressed in tobacco cells. Plant
799 Journal 8: 877-889
800 Maurer JB, Bacic A, Pereira-Netto AB, Donatti L, Zawadzki-Baggio SF, Pettolino FA
801 (2010) Arabinogalactan-proteins from cell suspension cultures of Araucaria
802 angustifolia. Phytochemistry 71: 1400-1409
803 Murata D, Nomura KH, Dejima K, Mizuguchi S, Kawasaki N, Matsuishi-Nakajima Y,
804 Ito S, Gengyo-Ando K, Kage-Nakadai E, Mitani S, Nomura K (2012)
805 GPI-anchor synthesis is indispensable for the germline development of the
806 nematode Caenorhabditis elegans. Mol Biol Cell 23: 982-995
807 Nagata T, Okada K, Takebe I, Matsui C (1981) Delivery of tobacco mosaic virus RNA
808 into plant protoplasts mediated by reverse-phase evaporation vesicles
809 (liposomes). Molecular & General Genetics 184: 161-165
810 Norman P, Wingate V, Fitter M, Lamb C (1986) Monoclonal-antibodies to plant
811 plasma-membrane antigens. Planta 167: 452-459
812 Oda Y, Asatsuma S, Nakasone H, Matsuoka K (2020) Sucrose starvation induces the
813 degradation of proteins in trans-Golgi network and secretory vesicle cluster in
814 tobacco BY-2 cells. Bioscience Biotechnology and Biochemistry 84: 1652-1666
815 Ogawa-Ohnishi M, Matsubayashi Y (2015) Identification of three potent
816 hydroxyproline O-galactosyltransferases in Arabidopsis. Plant J 81: 736-746
817 Oka T, Saito F, Shimma Y, Yoko-o T, Nomura Y, Matsuoka K, Jigami Y (2010)
818 Characterization of endoplasmic reticulum-localized UDP-D-galactose:
819 hydroxyproline O-galactosyltransferase using synthetic peptide substrates in
820 Arabidopsis. Plant Physiol 152: 332-340
821 Paris N, Rogers SW, Jiang L, Kirsch T, Beevers L, Phillips TE, Rogers JC (1997)
822 Molecular cloning and further characterization of a probable plant vacuolar
823 sorting receptor. Plant Physiol 115: 29-39
824 Parsons HT, Stevens TJ, McFarlane HE, Vidal-Melgosa S, Griss J, Lawrence N, Butler
825 R, Sousa MML, Salemi M, Willats WGT, Petzold CJ, Heazlewood JL, Lilley
826 KS (2019) Separating Golgi proteins from *cis* to *trans* reveals underlying
827 properties of cisternal localization. Plant Cell 31: 2010-2034
828 Pereira AM, Pereira LG, Coimbra S (2015) Arabinogalactan proteins: rising attention
829 from plant biologists. Plant Reprod 28: 1-15

bioRxiv preprint doi: https://doi.org/10.1101/2020.10.19.346049; this version posted October 19, 2020. The copyright holder for this preprint (which was not certified by peer review) is the author/funder. All rights reserved. No reuse allowed without permission.

Poulsen CP, Dilokpimol A, Geshi N (2015) Arabinogalactan biosynthesis: Implication of AtGALT29A enzyme activity regulated by phosphorylation and co-localized enzymes for nucleotide sugar metabolism in the compartments outside of the Golgi apparatus. Plant Signal Behav 10: e984524

Poulsen CP, Dilokpimol A, Mouille G, Burow M, Geshi N (2014) Arabinogalactan glycosyltransferases target to a unique subcellular compartment that may function in unconventional secretion in plants. Traffic 15: 1219-1234

Putoczki TL, Pettolino F, Griffin MD, Möller R, Gerrard JA, Bacic A, Jackson SL (2007) Characterization of the structure, expression and function of Pinus radiata D. Don arabinogalactan-proteins. Planta 226: 1131-1142

Sonobe S (1990) Cytochalasin B cytokinetic cleavage in miniprotoplast isolated from cultured tobacco cells. Protoplasma 155: 239-242

Shimizu M, Igasaki T, Yamada M, Yuasa K, Hasegawa J, Kato T, Tsukagoshi H, Nakamura K, Fukuda H, Matsuoka K (2005) Experimental determination of proline hydroxylation and hydroxyproline arabinogalactosylation motifs in secretory proteins. Plant J 42: 877-889

Showalter AM, Basu D (2016) Extensin and arabinogalactan-protein biosynthesis: Glycosyltransferases, research challenges, and biosensors. Front Plant Sci 7: 814

Showalter AM, Keppler B, Lichtenberg J, Gu D, Welch LR (2010) A bioinformatics approach to the identification, classification, and analysis of hydroxyproline-rich glycoproteins. Plant Physiol 153: 485-513

Singh H, Ansari HR, Raghava GP (2013) Improved method for linear B-cell epitope prediction using antigen's primary sequence. PLoS One 8: e62216

Steffan W, Kováčč P, Albersheim P, Darvill A, Hahn M (1995) Characterization of a monoclonal antibody that recognizes an arabinosylated (1-]6)-beta-D-galactan epitope in plant complex carbohydrates. Carbohydrate Research 275: 295-307

Suga S, Imagawa S, Maeshima M (2001) Specificity of the accumulation of mRNAs and proteins of the plasma membrane and tonoplast aquaporins in radish organs. Planta 212: 294-304

Tan L, Qiu F, Lamport DT, Kieliszewski MJ (2004) Structure of a hydroxyproline (Hyp)-arabinogalactan polysaccharide from repetitive Ala-Hyp expressed in transgenic Nicotiana tabacum. J Biol Chem 279: 13156-13165

Tan L, Varnai P, Lamport DT, Yuan C, Xu J, Qiu F, Kieliszewski MJ (2010) Plant O-hydroxyproline arabinogalactans are composed of repeating trigalactosyl subunits with short bifurcated side chains. J Biol Chem 285: 24575-24583

bioRxiv preprint doi: https://doi.org/10.1101/2020.10.19.346049; this version posted October 19, 2020. The copyright holder for this preprint (which was not certified by peer review) is the author/funder. All rights reserved. No reuse allowed without permission.

865 Tasaki M, Asatsuma S, Matsuoka K (2014) Monitoring protein turnover during
866 phosphate starvation-dependent autophagic degradation using a
867 photoconvertible fluorescent protein aggregate in tobacco BY-2 cells. Front
868 Plant Sci 5: 172
869 Temple H, Mortimer JC, Tryfona T, Yu X, Lopez-Hernandez F, Sorieul M, Anders N,
870 Dupree P (2019) Two members of the DUF579 family are responsible for
871 arabinogalactan methylation in Arabidopsis. Plant Direct 3: e00117
872 Toyooka K, Goto Y, Asatsuma S, Koizumi M, Mitsui T, Matsuoka K (2009) A mobile
873 secretory vesicle cluster involved in mass transport from the Golgi to the plant
874 cell exterior. Plant Cell 21: 1212-1229
875 Tryfona T, Liang HC, Kotake T, Tsumuraya Y, Stephens E, Dupree P (2012) Structural
876 characterization of Arabidopsis leaf arabinogalactan polysaccharides. Plant
877 Physiol 160: 653-666
878 Uemura T, Nakano RT, Takagi J, Wang Y, Kramer K, Finkemeier I, Nakagami H,
879 Tsuda K, Ueda T, Schulze-Lefert P, Nakano A (2019) A Golgi-released
880 subpopulation of the *trans*-Golgi network mediates protein secretion in
881 Arabidopsis. Plant Physiol 179: 519-532
882 Uemura T, Suda Y, Ueda T, Nakano A (2014) Dynamic behavior of the trans-golgi
883 network in root tissues of Arabidopsis revealed by super-resolution live imaging.
884 Plant Cell Physiol 55: 694-703
885 VandenBosch K, Bradley D, Knox J, Perotto S, Butcher G, Brewin N (1989) Common
886 components of the infection thread matrix and the intercellular space identified
887 by immunocytochemical analysis of pea nodules and uninfected roots. EMBO
888 Journal 8: 335-341
889 Velasquez SM, Ricardi MM, Poulsen CP, Oikawa A, Dilokpimol A, Halim A, Mangano
890 S, Denita Juarez SP, Marzol E, Salgado Salter JD, Dorosz JG, Borassi C, Möller
891 SR, Buono R, Ohsawa Y, Matsuoka K, Otegui MS, Scheller HV, Geshi N,
892 Petersen BL, Iusem ND, Estevez JM (2015) Complex regulation of
893 prolyl-4-hydroxylases impacts root hair expansion. Mol Plant 8: 734-746
894 Viotti C, Bubeck J, Stierhof YD, Krebs M, Langhans M, van den Berg W, van Dongen
895 W, Richter S, Geldner N, Takano J, Jürgens G, de Vries SC, Robinson DG,
896 Schumacher K (2010) Endocytic and secretory traffic in Arabidopsis merge in
897 the *trans*-Golgi network/early endosome, an independent and highly dynamic
898 organelle. Plant Cell 22: 1344-1357
899 Wilkop T, Pattathil S, Ren G, Davis DJ, Bao W, Duan D, Peralta AG, Domozych DS,
900 Hahn MG, Drakakaki G (2019) A hybrid approach enabling large-scale

bioRxiv preprint doi: https://doi.org/10.1101/2020.10.19.346049; this version posted October 19, 2020. The copyright holder for this preprint (which was not certified by peer review) is the author/funder. All rights reserved. No reuse allowed without permission.

glycomic analysis of post-Golgi vesicles reveals a transport route for polysaccharides. Plant Cell 31: 627-644

Xu J, Tan L, Lamport DT, Showalter AM, Kieliszewski MJ (2008) The O-Hyp glycosylation code in tobacco and Arabidopsis and a proposed role of Hyp-glycans in secretion. Phytochemistry 69: 1631-1640

Yamauchi N, Gosho T, Asatuma S, Toyooka K, Fujiwara T, Matsuoka K (2013) Polarized localization and borate-dependent degradation of the Arabidopsis borate transporter BOR1 in tobacco BY-2 cells. F1000Res 2: 185

Yates EA, Valdor JF, Haslam SM, Morris HR, Dell A, Mackie W, Knox JP (1996) Characterization of carbohydrate structural features recognized by anti-arabinogalactan-protein monoclonal antibodies. Glycobiology 6: 131-139

Yeats TH, Bacic A, Johnson KL (2018) Plant glycosylphosphatidylinositol anchored proteins at the plasma membrane-cell wall nexus. J Integr Plant Biol 60: 649-669

Yuasa K, Toyooka K, Fukuda H, Matsuoka K (2005) Membrane-anchored prolyl hydroxylase with an export signal from the endoplasmic reticulum. Plant J 41: 81-94

Legends to figures

Figure 1. Expression of the GFP-AGP fusion and its mutant without a GPI-anchoring signal in tobacco BY-2 cells. **A:** Schematic representation of the GFP fusion constructs. **B:** Accumulation of GFP fusion proteins in the culture of transformed tobacco cells. Total cell lysates were prepared from cells from 3-day-old and 7-day-old cultures, then separated by SDS-PAGE, and the GFP fluorescence in the gel was recorded. Each lane contained 3.6 μg of protein. **C:** Fractionation of 7-day-old cultures and distribution of the GFP-fusion proteins. Each lane contained proteins corresponding to 40 μL of cell culture. M, medium fraction; CW, cell wall fraction; Me, membrane fraction from total cell lysate; So, soluble fraction from total cell lysate.

Figure 2. Confocal localization study of GFP-AGP and GFP-AGPΔC in transformed tobacco BY-2 cells. **A:** Confocal image of 7-day-old transformed tobacco cells expressing GFP-AGP. **B:** Corresponding DIC image of cells in A. **C**: Confocal image of 7-day-old transformed tobacco cells expressing GFP-AGPΔC. **D:** Corresponding DIC image of cells in C. **E:** Confocal image of 7-day-old non-transformed cells. **F:**

bioRxiv preprint doi: https://doi.org/10.1101/2020.10.19.346049; this version posted October 19, 2020. The copyright holder for this preprint (which was not certified by peer review) is the author/funder. All rights reserved. No reuse allowed without permission.

Corresponding DIC image of cells in E. An identical condition was used to collect fluorescence images in A, C, and E. **G:** Confocal image of 7-day-old transformed tobacco cells expressing GFP-AGP after plasmolysis. **H–J:** Confocal image of 7-day-old transformed tobacco cells expressing GFP-AGP after staining with FM4-64. **H:** GFP fluorescence. **I:** FM4-64 fluorescence. **J:** merged image of H and I.

Figure 3. Expression, secretion and subcellular localization of the sporamin-AGP fusion protein and its mutant lacking a GPI-anchoring signal in tobacco BY-2 cells. **A:** Schematic representation of the sporamin fusion constructs. **B:** Expression and secretion of SPO-AGP and SPO-AGPΔC. 7-day-old cultures (Cu) of transformed BY-2 cells expressing SPO-AGP and SPO-AGPΔC and non-transformed BY-2 cells (WT) were separated into cells (C) and medium (M). The proteins in these fractions, corresponding to 10 μL of cell culture, were separated by SDS-PAGE, and sporamin-related polypeptides were detected by using an anti-SDS-denatured sporamin antibody. Closed arrowheads indicate transgene-dependent polypeptides. **C:** Detection of sporamin-related polypeptides after immunoprecipitation. Sporamin-related polypeptides were recovered by immunoprecipitation using immobilized anti-native sporamin, and the recovered proteins were analyzed by immunoblotting as described in the Materials and Methods section. Each lane contained sporamin-related polypeptides from a 0.5 ml, 7-day-old culture. Closed arrowheads indicate the migration position of transgene-dependent polypeptides detected in B. Open arrowheads indicate the calculated migration position of non-glycosylated polypeptides. **D:** Subcellular fractionation study of SPO-AGP-expressing cells. Fractionation of cells was carried out by differential centrifugation as described in the Materials and Methods section, and sporamin-related polypeptides in the fractions were recovered by immunoprecipitation, separated by SDS-PAGE, and detected by immunoblotting. P1, the 1,000*g* precipitate containing cell walls and unbroken cells; P10, the 10,000*g* precipitate containing most of the mitochondria; P100, the 100,000*g* precipitate containing microsomes; S, the 100,000*g* supernatant containing soluble proteins in the cytoplasm, vacuoles and periplasmic space. **E:** Subcellular fractionation study of SPO-AGPΔC-expressing cells. Subcellular fractionation and detection of sporamin-related polypeptides were carried out as in D.

Figure 4. Distribution of SPO-AGP within endomembrane organelles. Microsomes were prepared from SPO-AGP-expressing cells in the presence of Mg^{2+} (A) or EDTA (B) and subjected to isopycnic sucrose density gradient ultracentrifugation. The

bioRxiv preprint doi: https://doi.org/10.1101/2020.10.19.346049; this version posted October 19, 2020. The copyright holder for this preprint (which was not certified by peer review) is the author/funder. All rights reserved. No reuse allowed without permission.

973 resulting gradients were fractionated from the bottom into 17 fractions. The
974 concentration of sucrose in the gradient is shown at the top. The distribution of marker
975 proteins was analyzed by immunoblotting with specific antibodies: P-ATPase and PIP
976 for PM, Sec61 for the ER, GLMT1 for Golgi, and V-PPase for the vacuolar membrane.
977 The distribution of SPO-AGP, which migrated close to the top of the gel, was analyzed
978 by immunoblotting using an antibody against sporamin. The middle panels show the
979 relative distribution of SPO-AGP and marker proteins after quantification of the
980 signals on blots. The bottom panels are the results of immunoblots.
981
982 **Figure 5.** Distribution of different forms of SPO-AGPΔC in the cell. **A:** Distribution of
983 different forms in cells and protoplasts. Protoplasts were prepared from
984 SPO-AGPΔC-expressing cells by digesting the cell walls as described in the Materials
985 and Methods section. Proteins in cells and protoplasts were separated by SDS-PAGE
986 and sporamin-related polypeptides were detected by immunoblotting. As a control,
987 protoplasts were prepared from non-transformed cells (WT) and cross-reactive
988 polypeptides against anti-sporamin were analyzed by immunoblotting. Each lane
989 contained 25 μg protein. Closed arrowheads indicate the migration position of the
990 transgene-dependent polypeptides. Asterisk indicate a possible degradation product of
991 sporamin that was occasionally observed on immunoblots. **B:** Small SPO-AGPΔC was
992 localized in the vacuoles. To assess the localization of the intermediate and small
993 SPO-AGPΔC proteins, protoplasts were separated into vacuoplasts and cytoplasts and
994 the distribution of SPO-AGPΔC proteins were analyzed by immunoblotting. An equal
995 amount of the activity of α-mannosidase, which is a vacuolar marker enzyme, was
996 loaded in the vacuoplast and protoplast lanes, and nearly equal amounts of proteins
997 were loaded into the protoplast and cytoplast lanes. As a fractionation control,
998 mitochondrial porin was also detected by immunoblotting. **C,D:** Distribution of the
999 intermediate SPO-AGPΔC within endomembrane organelles. Microsomes were
1000 prepared from SPO-AGPΔC-expressing cells in the presence of Mg^{2+} (C) or EDTA
1001 (D), subjected to isopycnic sucrose density gradient ultracentrifugation, fractionated
1002 and analyzed for the distribution of intermediate SPO-AGPΔC and marker proteins as
1003 described in the legend to Fig. 4.
1004
1005 **Figure 6.** Both GFP-AGP and SPO-AGP are GPI-anchored proteins. **A:** Triton X-114
1006 two-phase partition assay of GFP-AGP, GFP-AGPΔC and PIP-GFP. Microsomes from
1007 GFP-AGP- or PIP-GFP-expressing cells, or the culture medium of
1008 GFP-AGPΔC-expressing cells was subjected to the two-phase separation assay as

bioRxiv preprint doi: https://doi.org/10.1101/2020.10.19.346049; this version posted October 19, 2020. The copyright holder for this preprint (which was not certified by peer review) is the author/funder. All rights reserved. No reuse allowed without permission.

described in the Materials and Methods section. Proteins in these two phases were separated by SDS-PAGE, and the fluorescence of GFP in the gel was recorded. Each lane contained proteins corresponding to an equal amount of microsomes or medium. aqu, aqueous phase; det, detergent phase. **B:** Triton X-114 two-phase partition assay of SPO-AGP and SPO-AGPΔC. Two-phase partition was carried out as in the legend to A. Proteins were separated by SDS-PAGE and detected by immunoblotting using anti-sporamin antibody. **C:** PI-PLC digestion of GFP-AGP. The two-phase partition assay was carried out in the absence and presence of PI-PLC. **D:** Two-phase partition assay of SPO-AGP. Microsomal proteins from SPO-AGP-expressing cells were subjected to the second-round two-phase partition assay in the absence or presence of PI-PLC. Both SPO-AGP and V-PPase, which is an integral membrane protein, were detected by immunoblotting. Each lane in these figures contained proteins corresponding to an equal amount of microsomes or medium.

Figure 7. The large form of SPO-AGPΔC was specifically recognized by LM2 monoclonal antibody. **A:** Detection by anti-sporamin antibody to show that nearly equal amount of sporamin-fusion proteins were loaded. **B:** Detection by the monoclonal antibody LM2, which recognizes a glycan epitope with β-linked glucuronic acid. **C:** Detection by the monoclonal antibody LM6, which recognizes a glycan epitope consisting of (1-5)-α-L-arabinosyl residues. AGP, microsomes from SPO-AGP-expressing cells; ΔC, culture medium from SPO-AGPΔC expressing culture; WT, corresponding microsomes and medium from non-transformed BY-2 cells with an equal amount of proteins with either microsomes from SPO-AGP or culture medium from SPO-AGPΔC.

bioRxiv preprint doi: https://doi.org/10.1101/2020.10.19.346049; this version posted October 19, 2020. The copyright holder for this preprint (which was not certified by peer review) is the author/funder. All rights reserved. No reuse allowed without permission.

Legends to the Supplemental figure and movie.

Supplemental figure 1.
Expression of the monomeric kikume green-red (mKikGR)-AGP fusion protein in tobacco BY-2 cells. Proteins were extracted from transformed tobacco BY-2 cells expressing either mKikGR-AGP, GFP or GFP-AGP and separated by SDS-PAGE. Then, the green fluorescence in the gel emitted from these proteins was recorded using a Typhoon 9600 image analyzer.

Supplemental movie 1.
Three-dimensional construction of the distribution of GFP-AGP fluorescence in transformed tobacco BY-2 cells. Z-stack images of green fluorescence were collected and reconstituted to the 3-D image. The constructed image was rotated.

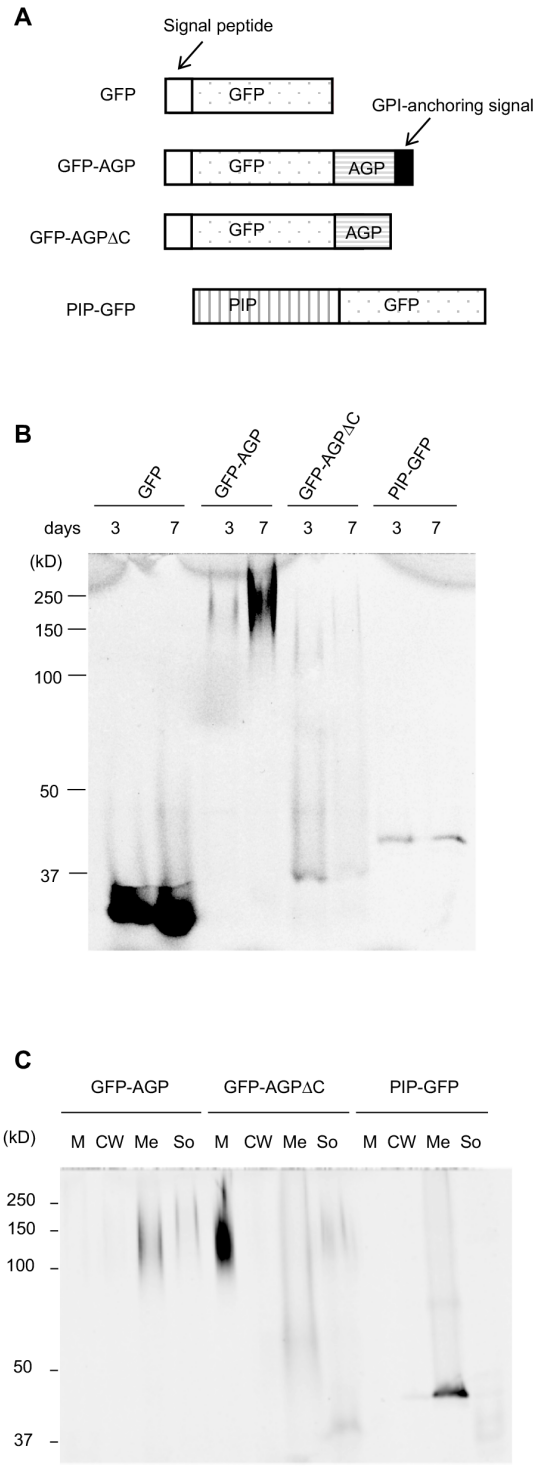

Figure 1. Expression of the GFP-AGP fusion and its mutant without a GPI-anchoring signal in tobacco BY-2 cells. A: Schematic representation of the GFP fusion constructs. B: Accumulation of GFP fusion proteins in the culture of transformed tobacco cells. Total cell lysates were prepared from cells from 3-day-old and 7-day-old cultures, then separated by SDS-PAGE, and the GFP fluorescence in the gel was recorded. Each lane contained 3.6 µg of protein. C: Fractionation of 7-day-old cultures and distribution of the GFP-fusion proteins. Each lane contained proteins corresponding to 40 µL of cell culture. M, medium fraction; CW, cell wall fraction; Me, membrane fraction from total cell lysate; So, soluble fraction from total cell lysate.

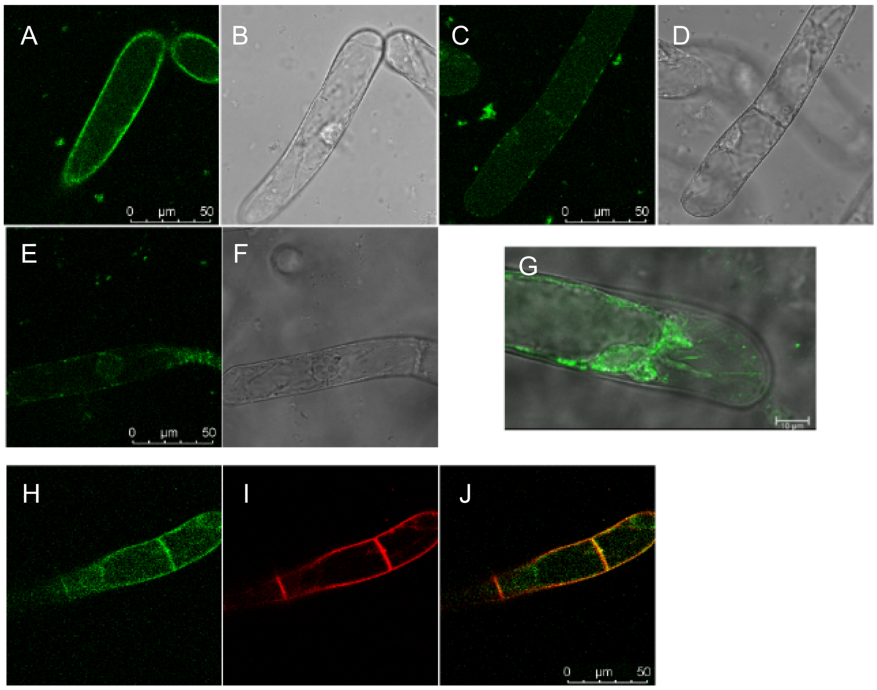

Figure 2. Confocal localization study of GFP-AGP and GFP-AGPΔC in transformed tobacco BY-2 cells. A: Confocal image of 7-day-old transformed tobacco cells expressing GFP-AGP. B: Corresponding DIC image of cells in A. C: Confocal image of 7-day-old transformed tobacco cells expressing GFP-AGPΔC. D: Corresponding DIC image of cells in C. E: Confocal image of 7-day-old non-transformed cells. F: Corresponding DIC image of cells in E. An identical condition was used to collect fluorescence images in A, C, and E. G: Confocal image of 7-day-old transformed tobacco cells expressing GFP-AGP after plasmolysis. H–J: Confocal image of 7-day-old transformed tobacco cells expressing GFP-AGP after staining with FM4-64. H: GFP fluorescence. I: FM4-64 fluorescence. J: merged image of H and I.

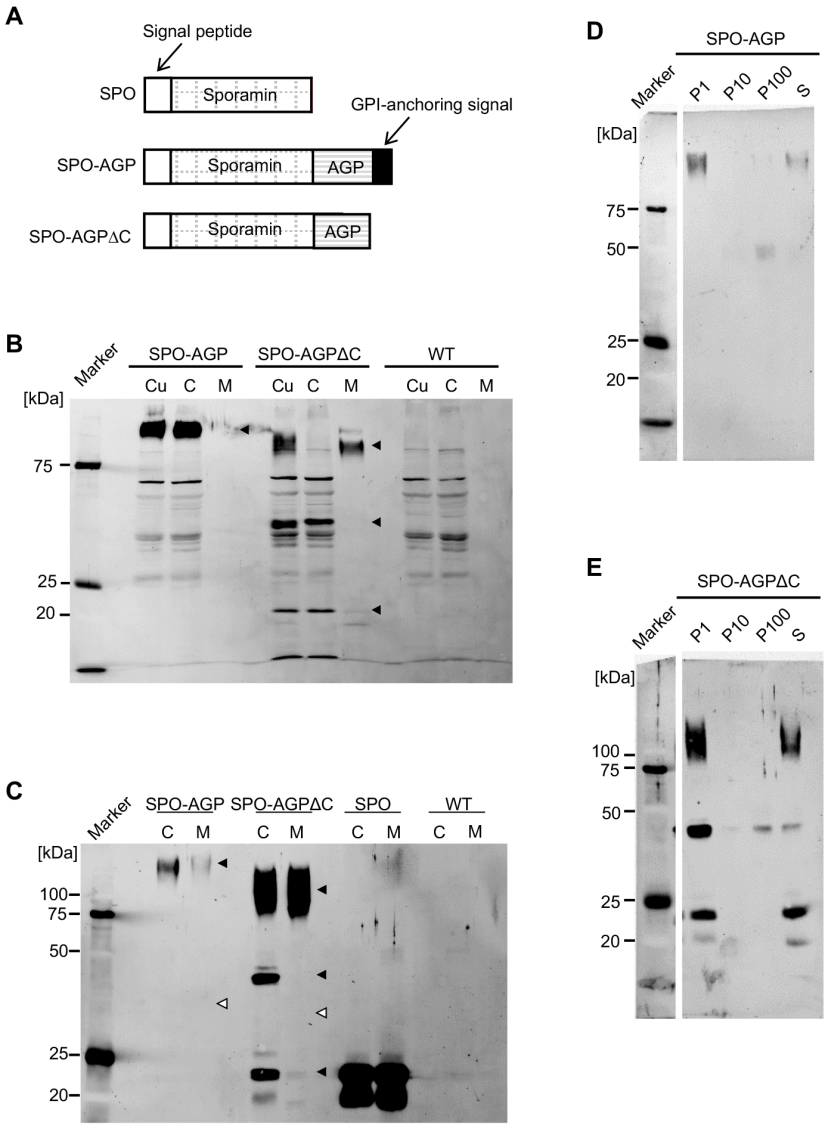

Figure 3. Expression, secretion and subcellular localization of the sporamin-AGP fusion protein and its mutant lacking a GPI-anchoring signal in tobacco BY-2 cells. A: Schematic representation of the sporamin fusion constructs. B: Expression and secretion of SPO-AGP and SPO-AGPΔC. 7-day-old cultures (Cu) of transformed BY-2 cells expressing SPO-AGP and SPO-AGPΔC and non-transformed BY-2 cells (WT) were separated into cells (C) and medium (M). The proteins in these fractions, corresponding to 10 μL of cell culture, were separated by SDS-PAGE, and sporamin-related polypeptides were detected by using an anti-SDS-denatured sporamin antibody. Closed arrowheads indicate transgene-dependent polypeptides. C: Detection of sporamin-related polypeptides after immunoprecipitation. Sporamin-related polypeptides were recovered by immunoprecipitation using immobilized anti-native sporamin, and the recovered proteins were analyzed by immunoblotting as described in the Materials and Methods section. Each lane contained sporamin-related polypeptides from a 0.5 ml, 7-day-old culture. Closed arrowheads indicate the migration position of transgene-dependent polypeptides detected in B. Open arrowheads indicate the calculated migration position of non-glycosylated polypeptides. D: Subcellular fractionation study of SPO-AGP-expressing cells. Fractionation of cells was carried out by differential centrifugation as described in the Materials and Methods section, and sporamin-related polypeptides in the fractions were recovered by immunoprecipitation, separated by SDS-PAGE, and detected by immunoblotting. P1, the 1,000g precipitate containing cell walls and unbroken cells; P10, the 10,000g precipitate containing most of the mitochondria; P100, the 100,000g precipitate containing microsomes; S, the 100,000g supernatant containing soluble proteins in the cytoplasm, vacuoles and periplasmic space. E: Subcellular fractionation study of SPO-AGPΔC-expressing cells. Subcellular fractionation and detection of sporamin-related polypeptides were carried out as in D.

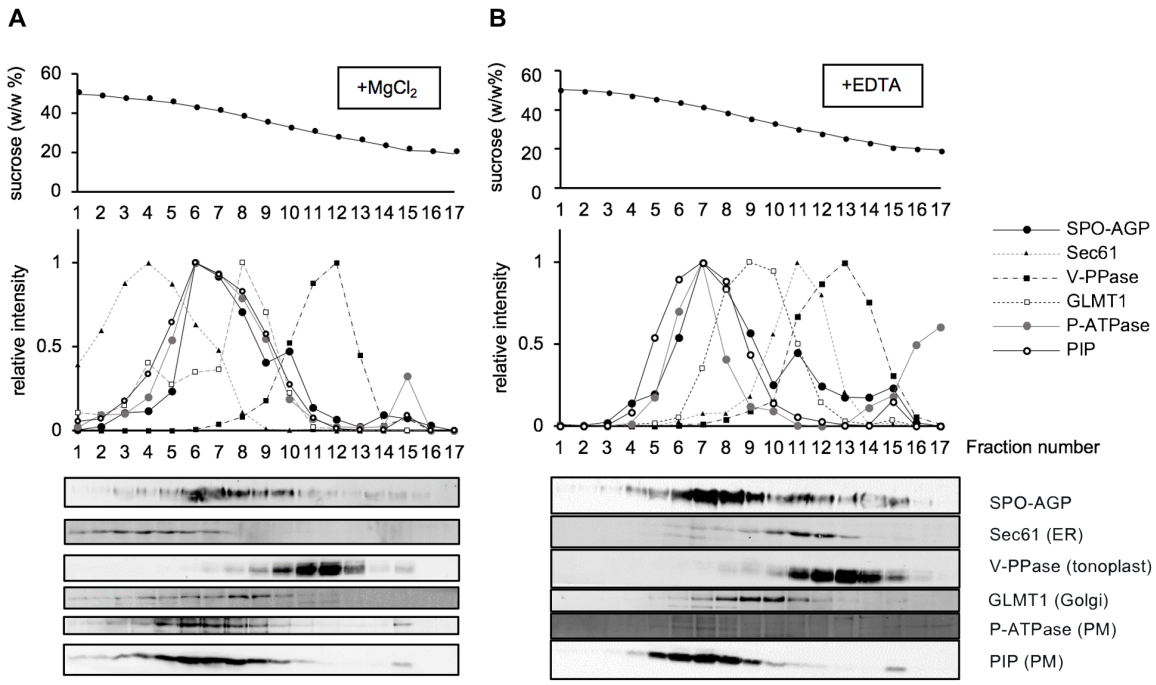

Figure 4. Distribution of SPO-AGP within endomembrane organelles. Microsomes were prepared from SPO-AGP-expressing cells in the presence of Mg2+ (A) or EDTA (B) and subjected to isopycnic sucrose density gradient ultracentrifugation. The resulting gradients were fractionated from the bottom into 17 fractions. The concentration of sucrose in the gradient is shown at the top. The distribution of marker proteins was analyzed by immunoblotting with specific antibodies: P-ATPase and PIP for PM, Sec61 for the ER, GLMT1 for Golgi, and V-PPase for the vacuolar membrane. The distribution of SPO-AGP, which migrated close to the top of the gel, was analyzed by immunoblotting using an antibody against sporamin. The middle panels show the relative distribution of SPO-AGP and marker proteins after quantification of the signals on blots. The bottom panels are the results of immunoblots.

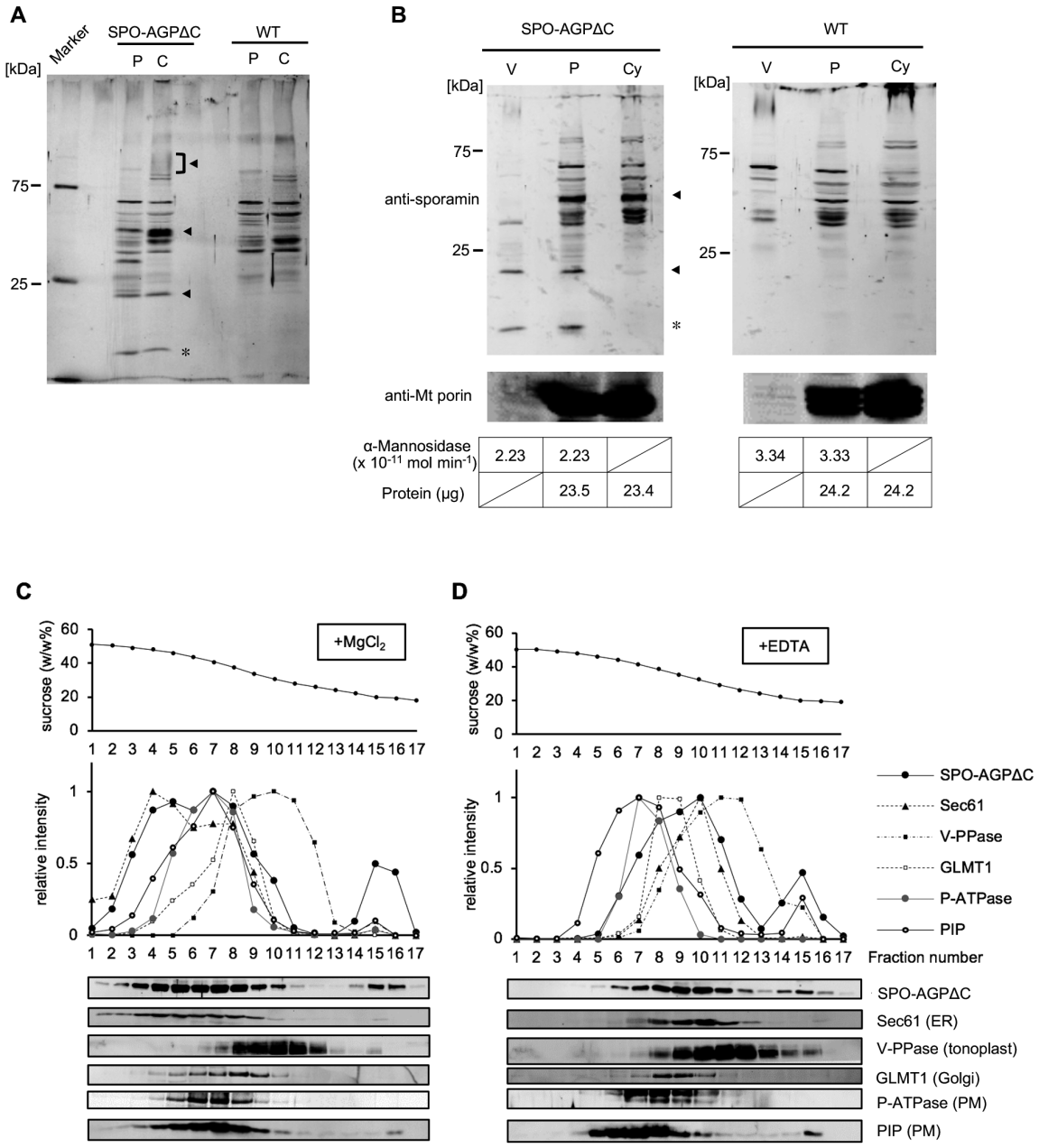

Figure 5. Distribution of different forms of SPO-AGPΔC in the cell. A: Distribution of different forms in cells and protoplasts. Protoplasts were prepared from SPO-AGPΔC-expressing cells by digesting the cell walls as described in the Materials and Methods section. Proteins in cells and protoplasts were separated by SDS-PAGE and sporamin-related polypeptides were detected by immunoblotting. As a control, protoplasts were prepared from non-transformed cells (WT) and cross-reactive polypeptides against anti-sporamin were analyzed by immunoblotting. Each lane contained 25 μg protein. Closed arrowheads indicate the migration position of the transgene-dependent polypeptides. Asterisk indicate a possible degradation product of sporamin that was occasionally observed on immunoblots. B: Small SPO-AGPΔC was localized in the vacuoles. To assess the localization of the intermediate and small SPO-AGPΔC proteins, protoplasts were separated into vacuoplasts and cytoplasts and the distribution of SPO-AGPΔC proteins were analyzed by immunoblotting. An equal amount of the activity of α-mannosidase, which is a vacuolar marker enzyme, was loaded in the vacuoplast and protoplast lanes, and nearly equal amounts of proteins were loaded into the protoplast and cytoplast lanes. As a fractionation control, mitochondrial porin was also detected by immunoblotting. C,D: Distribution of the intermediate SPO-AGPΔC within endomembrane organelles. Microsomes were prepared from SPO-AGPΔC-expressing cells in the presence of Mg2+ (C) or EDTA (D), subjected to isopycnic sucrose density gradient ultracentrifugation, fractionated and analyzed for the distribution of intermediate SPO-AGPΔC and marker proteins as described in the legend to Fig. 4.

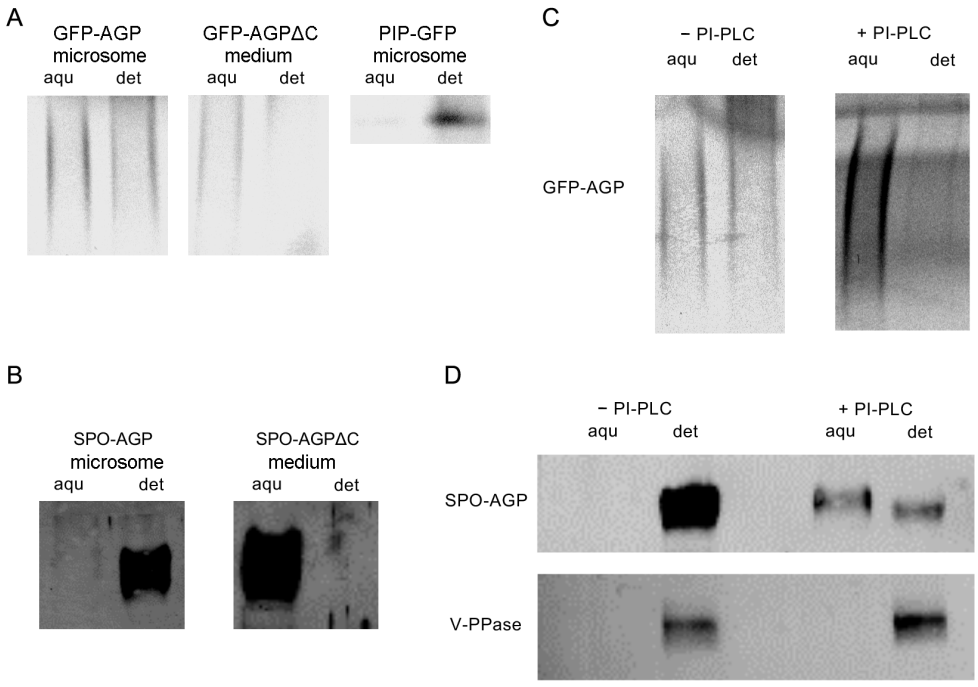

Figure 6. Both GFP-AGP and SPO-AGP are GPI-anchored proteins. A: Triton X-114 two-phase partition assay of GFP-AGP, GFP-AGPΔC and PIP-GFP. Microsomes from GFP-AGP- or PIP-GFP-expressing cells, or the culture medium of GFP-AGPΔC-expressing cells was subjected to the two-phase separation assay as described in the Materials and Methods section. Proteins in these two phases were separated by SDS-PAGE, and the fluorescence of GFP in the gel was recorded. Each lane contained proteins corresponding to an equal amount of microsomes or medium. aqu, aqueous phase; det, detergent phase. B: Triton X-114 two-phase partition assay of SPO-AGP and SPO-AGPΔC. Two-phase partition was carried out as in the legend to A. Proteins were separated by SDS-PAGE and detected by immunoblotting using anti-sporamin antibody. C: PI-PLC digestion of GFP-AGP. The two-phase partition assay was carried out in the absence and presence of PI-PLC. D: Two-phase partition assay of SPO-AGP. Microsomal proteins from SPO-AGP-expressing cells were subjected to the second-round two-phase partition assay in the absence or presence of PI-PLC. Both SPO-AGP and V-PPase, which is an integral membrane protein, were detected by immunoblotting. Each lane in these figures contained proteins corresponding to an equal amount of microsomes or medium.

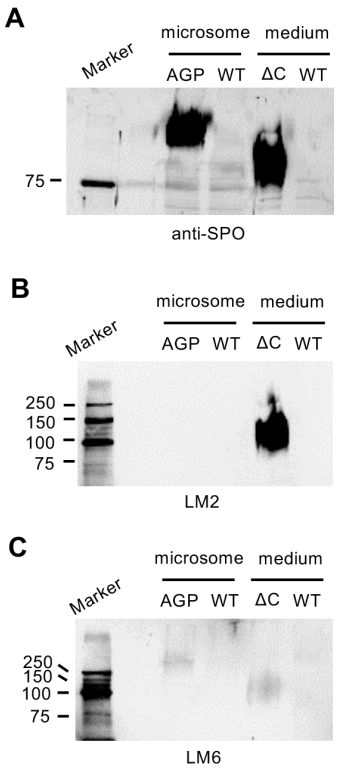

Figure 7. The large form of SPO-AGPΔC was specifically recognized by LM2 monoclonal antibody. A: Detection by anti-sporamin antibody to show that nearly equal amount of sporamin-fusion proteins were loaded. B: Detection by the monoclonal antibody LM2, which recognizes a glycan epitope with β-linked glucuronic acid. C: Detection by the monoclonal antibody LM6, which recognizes a glycan epitope consisting of (1-5)-α-L-arabinosyl residues. AGP, microsomes from SPO-AGP-expressing cells; ΔC, culture medium from SPO-AGPΔC expressing culture; WT, corresponding microsomes and medium from non-transformed BY-2 cells with an equal amount of proteins with either microsomes from SPO-AGP or culture medium from SPO-AGPΔC.

Parsed Citations

Abiodun MO, Matsuoka K (2013) Evidence that proliferation of Golgi apparatus depends on both de novo generation from the endoplasmic reticulum and formation from pre-existing stacks during the growth of tobacco BY-2 cells. Plant Cell Physiol 54: 541-554
Google Scholar: Author Only Title Only Author and Title

Basu D, Liang Y, Liu X, Himmeldirk K, Faik A, Kieliszewski M, Held M, Showalter AM (2013) Functional identification of a hydroxyproline-O-galactosyltransferase specific for arabinogalactan protein biosynthesis in Arabidopsis. J Biol Chem 288: 10132-10143
Google Scholar: Author Only Title Only Author and Title

Basu D, Wang W, Ma S, DeBrosse T, Poirier E, Emch K, Soukup E, Tian L, Showalter AM (2015) Two hydroxyproline galactosyltransferases, GALT5 and GALT2, function in arabinogalactan-protein glycosylation, growth and development in Arabidopsis. PLoS One 10: e0125624
Google Scholar: Author Only Title Only Author and Title

Boller T, Kende H (1979) Hydrolytic enzymes in the central vacuole of plant cells. Plant Physiol 63: 1123-1132
Google Scholar: Author Only Title Only Author and Title

Bordier C (1981) Phase separation of integral membrane proteins in Triton X-114 solution. J Biol Chem 256: 1604-1607
Google Scholar: Author Only Title Only Author and Title

Chiu W, Niwa Y, Zeng W, Hirano T, Kobayashi H, Sheen J (1996) Engineered GFP as a vital reporter in plants. Curr Biol 6: 325-330
Google Scholar: Author Only Title Only Author and Title

De Caroli M, Lenucci MS, Di Sansebastiano GP, Dalessandro G, De Lorenzo G, Piro G (2011) Protein trafficking to the cell wall occurs through mechanisms distinguishable from default sorting in tobacco. Plant J 65: 295-308
Google Scholar: Author Only Title Only Author and Title

Dilokpimol A, Poulsen CP, Vereb G, Kaneko S, Schulz A, Geshi N (2014) Galactosyltransferases from Arabidopsis thaliana in the biosynthesis of type II arabinogalactan: molecular interaction enhances enzyme activity. BMC Plant Biol 14: 90
Google Scholar: Author Only Title Only Author and Title

Drakakaki G, van de Ven W, Pan S, Miao Y, Wang J, Keinath NF, Weatherly B, Jiang L, Schumacher K, Hicks G, Raikhel N (2012) Isolation and proteomic analysis of the SYP61 compartment reveal its role in exocytic trafficking in Arabidopsis. Cell Res 22: 413-424
Google Scholar: Author Only Title Only Author and Title

Du H, Simpson RJ, Moritz RL, Clarke AE, Bacic A (1994) Isolation of the protein backbone of an arabinogalactan-protein from the styles of Nicotiana alata and characterization of a corresponding cDNA. Plant Cell 6: 1643-1653
Google Scholar: Author Only Title Only Author and Title

Emans N, Zimmermann S, Fischer R (2002) Uptake of a fluorescent marker in plant cells is sensitive to brefeldin A and wortmannin. Plant Cell 14: 71-86
Google Scholar: Author Only Title Only Author and Title

Gális I, Simek P, Narisawa T, Sasaki M, Horiguchi T, Fukuda H, Matsuoka K (2006) A novel R2R3 MYB transcription factor NtMYBJS1 is a methyl jasmonate-dependent regulator of phenylpropanoid-conjugate biosynthesis in tobacco. Plant J 46: 573-592
Google Scholar: Author Only Title Only Author and Title

Habuchi S, Tsutsui H, Kochaniak AB, Miyawaki A, van Oijen AM (2008) mKikGR, a monomeric photoswitchable fluorescent protein. PLoS One 3: e3944
Google Scholar: Author Only Title Only Author and Title

Hong E, Davidson AR, Kaiser CA (1996) A pathway for targeting soluble misfolded proteins to the yeast vacuole. J Cell Biol 135: 623-633
Google Scholar: Author Only Title Only Author and Title

Hooper NM (2001) Determination of glycosyl-phosphatidylinositol membrane protein anchorage. Proteomics 1: 748-755
Google Scholar: Author Only Title Only Author and Title

Kang BH, Nielsen E, Preuss ML, Mastronarde D, Staehelin LA (2011) Electron tomography of RabA4b- and PI-4Kβ1-labeled trans Golgi network compartments in Arabidopsis. Traffic 12: 313-329
Google Scholar: Author Only Title Only Author and Title

Knoch E, Dilokpimol A, Tryfona T, Poulsen CP, Xiong G, Harholt J, Petersen BL, Ulvskov P, Hadi MZ, Kotake T, Tsumuraya Y, Pauly M, Dupree P, Geshi N (2013) A β-glucuronosyltransferase from Arabidopsis thaliana involved in biosynthesis of type II arabinogalactan has a role in cell elongation during seedling growth. Plant J 76: 1016-1029
Google Scholar: Author Only Title Only Author and Title

Lind JL, Bacic A, Clarke AE, Anderson MA (1994) A style-specific hydroxyproline-rich glycoprotein with properties of both extensins and arabinogalactan proteins. Plant J 6: 491-502
Google Scholar: Author Only Title Only Author and Title

Liu J, Hayashi K, Matsuoka K (2015) Membrane topology of Golgi-localized probable S-adenosylmethionine-dependent methyltransferase in tobacco (Nicotiana tabacum) BY-2 cells. Biosci Biotechnol Biochem 79: 2007-2013

Google Scholar: Author Only Title Only Author and Title

Liu YS, Fujita M (2020) Mammalian GPI-anchor modifications and the enzymes involved. Biochem Soc Trans 48: 1129-1138
Google Scholar: Author Only Title Only Author and Title

Matsuoka K, Demura T, Galis I, Horiguchi T, Sasaki M, Tashiro G, Fukuda H (2004) A comprehensive gene expression analysis toward the understanding of growth and differentiation of tobacco BY-2 cells. Plant and Cell Physiology 45: 1280-1289
Google Scholar: Author Only Title Only Author and Title

Matsuoka K, Higuchi T, Maeshima M, Nakamura K (1997) A Vacuolar-Type H+-ATPase in a nonvacuolar organelle is required for the sorting of soluble vacuolar protein precursors in tobacco cells. Plant Cell 9: 533-546
Google Scholar: Author Only Title Only Author and Title

Matsuoka K, Nakamura K (1991) Propeptide of a precursor to a plant vacuolar protein required for vacuolar targeting. Proc Natl Acad Sci U S A 88: 834-838
Google Scholar: Author Only Title Only Author and Title

Matsuoka K, Nakamura K (1999) Large alkyl side-chains of isoleucine and leucine in the NPIRL region constitute the core of the vacuolar sorting determinant of sporamin precursor. Plant Mol Biol 41: 825-835
Google Scholar: Author Only Title Only Author and Title

Matsuoka K, Watanabe N, Nakamura K (1995) O-glycosylation of a precursor to a sweet potato vacuolar protein, sporamin, expressed in tobacco cells. Plant Journal 8: 877-889
Google Scholar: Author Only Title Only Author and Title

Maurer JB, Bacic A, Pereira-Netto AB, Donatti L, Zawadzki-Baggio SF, Pettolino FA (2010) Arabinogalactan-proteins from cell suspension cultures of Araucaria angustifolia. Phytochemistry 71: 1400-1409
Google Scholar: Author Only Title Only Author and Title

Murata D, Nomura KH, Dejima K, Mizuguchi S, Kawasaki N, Matsuishi-Nakajima Y, Ito S, Gengyo-Ando K, Kage-Nakadai E, Mitani S, Nomura K (2012) GPI-anchor synthesis is indispensable for the germline development of the nematode Caenorhabditis elegans. Mol Biol Cell 23: 982-995
Google Scholar: Author Only Title Only Author and Title

Nagata T, Okada K, Takebe I, Matsui C (1981) Delivery of tobacco mosaic virus RNA into plant protoplasts mediated by reverse-phase evaporation vesicles (liposomes). Molecular & General Genetics 184: 161-165
Google Scholar: Author Only Title Only Author and Title

Norman P, Wingate V, Fitter M, Lamb C (1986) Monoclonal-antibodies to plant plasma-membrane antigens. Planta 167: 452-459
Google Scholar: Author Only Title Only Author and Title

Oda Y, Asatsuma S, Nakasone H, Matsuoka K (2020) Sucrose starvation induces the degradation of proteins in trans-Golgi network and secretory vesicle cluster in tobacco BY-2 cells. Bioscience Biotechnology and Biochemistry 84: 1652-1666
Google Scholar: Author Only Title Only Author and Title

Ogawa-Ohnishi M, Matsubayashi Y (2015) Identification of three potent hydroxyproline O-galactosyltransferases in Arabidopsis. Plant J 81: 736-746
Google Scholar: Author Only Title Only Author and Title

Oka T, Saito F, Shimma Y, Yoko-o T, Nomura Y, Matsuoka K, Jigami Y (2010) Characterization of endoplasmic reticulum-localized UDP-D-galactose: hydroxyproline O-galactosyltransferase using synthetic peptide substrates in Arabidopsis. Plant Physiol 152: 332-340
Google Scholar: Author Only Title Only Author and Title

Paris N, Rogers SW, Jiang L, Kirsch T, Beevers L, Phillips TE, Rogers JC (1997) Molecular cloning and further characterization of a probable plant vacuolar sorting receptor. Plant Physiol 115: 29-39
Google Scholar: Author Only Title Only Author and Title

Parsons HT, Stevens TJ, McFarlane HE, Vidal-Melgosa S, Griss J, Lawrence N, Butler R, Sousa MML, Salemi M, Willats WGT, Petzold CJ, Heazlewood JL, Lilley KS (2019) Separating Golgi proteins from cis to trans reveals underlying properties of cisternal localization. Plant Cell 31: 2010-2034
Google Scholar: Author Only Title Only Author and Title

Pereira AM, Pereira LG, Coimbra S (2015) Arabinogalactan proteins: rising attention from plant biologists. Plant Reprod 28: 1-15
Google Scholar: Author Only Title Only Author and Title

Poulsen CP, Dilokpimol A, Geshi N (2015) Arabinogalactan biosynthesis: Implication of AtGALT29A enzyme activity regulated by phosphorylation and co-localized enzymes for nucleotide sugar metabolism in the compartments outside of the Golgi apparatus. Plant Signal Behav 10: e984524
Google Scholar: Author Only Title Only Author and Title

Poulsen CP, Dilokpimol A, Mouille G, Burow M, Geshi N (2014) Arabinogalactan glycosyltransferases target to a unique subcellular compartment that may function in unconventional secretion in plants. Traffic 15: 1219-1234
Google Scholar: Author Only Title Only Author and Title

Putoczki TL, Pettolino F, Griffin MD, Möller R, Gerrard JA, Bacic A, Jackson SL (2007) Characterization of the structure, expression and function of Pinus radiata D. Don arabinogalactan-proteins. Planta 226: 1131-1142
Google Scholar: Author Only Title Only Author and Title

Sonobe S (1990) Cytochalasin B cytokinetic cleavage in miniprotoplast isolated from cultured tobacco cells. Protoplasma 155: 239-242
Google Scholar: Author Only Title Only Author and Title

Shimizu M, Igasaki T, Yamada M, Yuasa K, Hasegawa J, Kato T, Tsukagoshi H, Nakamura K, Fukuda H, Matsuoka K (2005) Experimental determination of proline hydroxylation and hydroxyproline arabinogalactosylation motifs in secretory proteins. Plant J 42: 877-889
Google Scholar: Author Only Title Only Author and Title

Showalter AM, Basu D (2016) Extensin and arabinogalactan-protein biosynthesis: Glycosyltransferases, research challenges, and biosensors. Front Plant Sci 7: 814
Google Scholar: Author Only Title Only Author and Title

Showalter AM, Keppler B, Lichtenberg J, Gu D, Welch LR (2010) A bioinformatics approach to the identification, classification, and analysis of hydroxyproline-rich glycoproteins. Plant Physiol 153: 485-513
Google Scholar: Author Only Title Only Author and Title

Singh H, Ansari HR, Raghava GP (2013) Improved method for linear B-cell epitope prediction using antigen's primary sequence. PLoS One 8: e62216
Google Scholar: Author Only Title Only Author and Title

Steffan W, Kovácč P, Albersheim P, Darvill A, Hahn M (1995) Characterization of a monoclonal antibody that recognizes an arabinosylated (1-]6)-beta-D-galactan epitope in plant complex carbohydrates. Carbohydrate Research 275: 295-307
Google Scholar: Author Only Title Only Author and Title

Suga S, Imagawa S, Maeshima M (2001) Specificity of the accumulation of mRNAs and proteins of the plasma membrane and tonoplast aquaporins in radish organs. Planta 212: 294-304
Google Scholar: Author Only Title Only Author and Title

Tan L, Qiu F, Lamport DT, Kieliszewski MJ (2004) Structure of a hydroxyproline (Hyp)-arabinogalactan polysaccharide from repetitive Ala-Hyp expressed in transgenic Nicotiana tabacum. J Biol Chem 279: 13156-13165
Google Scholar: Author Only Title Only Author and Title

Tan L, Varnai P, Lamport DT, Yuan C, Xu J, Qiu F, Kieliszewski MJ (2010) Plant O-hydroxyproline arabinogalactans are composed of repeating trigalactosyl subunits with short bifurcated side chains. J Biol Chem 285: 24575-24583
Google Scholar: Author Only Title Only Author and Title

Tasaki M, Asatsuma S, Matsuoka K (2014) Monitoring protein turnover during phosphate starvation-dependent autophagic degradation using a photoconvertible fluorescent protein aggregate in tobacco BY-2 cells. Front Plant Sci 5: 172
Google Scholar: Author Only Title Only Author and Title

Temple H, Mortimer JC, Tryfona T, Yu X, Lopez-Hernandez F, Sorieul M, Anders N, Dupree P (2019) Two members of the DUF579 family are responsible for arabinogalactan methylation in Arabidopsis. Plant Direct 3: e00117
Google Scholar: Author Only Title Only Author and Title

Toyooka K, Goto Y, Asatsuma S, Koizumi M, Mitsui T, Matsuoka K (2009) A mobile secretory vesicle cluster involved in mass transport from the Golgi to the plant cell exterior. Plant Cell 21: 1212-1229
Google Scholar: Author Only Title Only Author and Title

Tryfona T, Liang HC, Kotake T, Tsumuraya Y, Stephens E, Dupree P (2012) Structural characterization of Arabidopsis leaf arabinogalactan polysaccharides. Plant Physiol 160: 653-666
Google Scholar: Author Only Title Only Author and Title

Uemura T, Nakano RT, Takagi J, Wang Y, Kramer K, Finkemeier I, Nakagami H, Tsuda K, Ueda T, Schulze-Lefert P, Nakano A (2019) A Golgi-released subpopulation of the trans-Golgi network mediates protein secretion in Arabidopsis. Plant Physiol 179: 519-532
Google Scholar: Author Only Title Only Author and Title

Uemura T, Suda Y, Ueda T, Nakano A (2014) Dynamic behavior of the trans-golgi network in root tissues of Arabidopsis revealed by super-resolution live imaging. Plant Cell Physiol 55: 694-703
Google Scholar: Author Only Title Only Author and Title

VandenBosch K, Bradley D, Knox J, Perotto S, Butcher G, Brewin N (1989) Common components of the infection thread matrix and the intercellular space identified by immunocytochemical analysis of pea nodules and uninfected roots. EMBO Journal 8: 335-341
Google Scholar: Author Only Title Only Author and Title

Velasquez SM, Ricardi MM, Poulsen CP, Oikawa A, Dilokpimol A, Halim A, Mangano S, Denita Juarez SP, Marzol E, Salgado Salter JD, Dorosz JG, Borassi C, Möller SR, Buono R, Ohsawa Y, Matsuoka K, Otegui MS, Scheller HV, Geshi N, Petersen BL, Iusem ND, Estevez JM (2015) Complex regulation of prolyl-4-hydroxylases impacts root hair expansion. Mol Plant 8: 734-746
Google Scholar: Author Only Title Only Author and Title

Viotti C, Bubeck J, Stierhof YD, Krebs M, Langhans M, van den Berg W, van Dongen W, Richter S, Geldner N, Takano J, Jürgens G, de Vries SC, Robinson DG, Schumacher K (2010) Endocytic and secretory traffic in Arabidopsis merge in the trans-Golgi network/early

endosome, an independent and highly dynamic organelle. Plant Cell 22: 1344-1357
Google Scholar: Author Only Title Only Author and Title

Wilkop T, Pattathil S, Ren G, Davis DJ, Bao W, Duan D, Peralta AG, Domozych DS, Hahn MG, Drakakaki G (2019) A hybrid approach enabling large-scale glycomic analysis of post-Golgi vesicles reveals a transport route for polysaccharides. Plant Cell 31: 627-644
Google Scholar: Author Only Title Only Author and Title

Xu J, Tan L, Lamport DT, Showalter AM, Kieliszewski MJ (2008) The O-Hyp glycosylation code in tobacco and Arabidopsis and a proposed role of Hyp-glycans in secretion. Phytochemistry 69: 1631-1640
Google Scholar: Author Only Title Only Author and Title

Yamauchi N, Gosho T, Asatuma S, Toyooka K, Fujiwara T, Matsuoka K (2013) Polarized localization and borate-dependent degradation of the Arabidopsis borate transporter BOR1 in tobacco BY-2 cells. F1000Res 2: 185
Google Scholar: Author Only Title Only Author and Title

Yates EA, Valdor JF, Haslam SM, Morris HR, Dell A, Mackie W, Knox JP (1996) Characterization of carbohydrate structural features recognized by anti-arabinogalactan-protein monoclonal antibodies. Glycobiology 6: 131-139
Google Scholar: Author Only Title Only Author and Title

Yeats TH, Bacic A, Johnson KL (2018) Plant glycosylphosphatidylinositol anchored proteins at the plasma membrane-cell wall nexus. J Integr Plant Biol 60: 649-669
Google Scholar: Author Only Title Only Author and Title

Yuasa K, Toyooka K, Fukuda H, Matsuoka K (2005) Membrane-anchored prolyl hydroxylase with an export signal from the endoplasmic reticulum. Plant J 41: 81-94
Google Scholar: Author Only Title Only Author and Title